Calibration of Local-Stochastic Volatility Models by Optimal Transport

Ivan Guo^{1,2}, Grégoire Loeper^{1,2}, and Shiyi Wang¹

¹School of Mathematics, Monash University, Australia ²Centre for Quantitative Finance and Investment Strategies, Monash University, Australia

October 27, 2020

Abstract

In this paper, we study a semi-martingale optimal transport problem and its application to the calibration of Local-Stochastic Volatility (LSV) models. Rather than considering the classical constraints on marginal distributions at initial and final time, we optimise our cost function given the prices of a finite number of European options. We formulate the problem as a convex optimisation problem, for which we provide a PDE formulation along with its dual counterpart. Then we solve numerically the dual problem, which involves a fully non-linear Hamilton–Jacobi–Bellman equation. The method is tested by calibrating a Heston-like LSV model with simulated data and foreign exchange market data.

Keywords. optimal transport, duality theory, local-stochastic volatility, calibration **AMS subject classifications.** 91G20, 91G80, 60H30

1 Introduction

Since the introduction of the Black–Scholes model, a lot of effort has been put on developing sophisticated volatility models that properly capture the market dynamics. In the space of equities and currencies, the most widely used models are the Local Volatility (LV) model by Dupire (1994) and the Stochastic Volatility (SV) models (see e.g., Gatheral, 2011; Heston, 1993). Introduced as an extension of the Black–Scholes model, the LV model can be exactly calibrated to any arbitrage-free implied volatility surface. Despite this feature, the LV model has often been criticised for its unrealistic volatility dynamics. The SV models tend to be more consistent with the market dynamics, but they struggle to fit short term market smiles and skews, and being parametric, they do not have enough degrees of freedom to match all vanilla market prices. A better fit can be obtained by increasing the number of stochastic factors in the SV models; however, this also increases the complexity of calibration and pricing.

Local-Stochastic Volatility (LSV) models, introduced in Jex et al. (1999), naturally extend and take advantage of both approaches. The idea behind LSV models is to incorporate a local, non-parametric, factor into the SV models. Thus, while keeping consistent dynamics, the model

can match all observed market prices (as long as one restricts to European claims). The determination of this local factor (also called *leverage*) is based on the mimicking theorem by Gyöngy (1986). Research into the numerical calibration of LSV models has been developed in two different directions. One is based on a Monte Carlo approach, with Henry-Labordere (2009), followed by Guyon and Henry-Labordere (2011) using a so-called McKean's particle method. Another approach relies on solving the Fokker–Planck equation as in Ren et al. (2007). Engelmann et al. (2011) used the finite volume method (FVM) to solve the partial differential equation (PDE), while Tian et al. (2015) considered time-dependent parameters. In a more recent study, Wyns and Du Toit (2017) considered a method that combines the FVM with alternating direction implicit (ADI) schemes.

All of the calibration methods mentioned above require a priori knowledge of the Local Volatility surface. This is usually obtained by using Dupire's formula (Dupire, 1994) assuming the knowledge of vanilla options for all strikes and maturities. However, only a finite number of options are available in practice. Thus, an interpolation of the implied volatility surface or option prices is often needed, which can lead to inaccuracies and instabilities. Inaccuracies can come from the usage of a parametric model for the volatility surface that will not match perfectly market prices by definition. Instabilities can come form the interpolating model being not arbitrage-free. It also raises the question of what arbitrary shape of extrapolation one is going to take for very out of the money strikes. Moreover, there is no a priori control on the regularity of the leverage function, and even its very existence remains an open problem, although some results for small times have been obtained in Abergel and Tachet (2010) (cf. Saporito et al., 2019, for an application of Tikhonov regularisation technique to the LSV calibration problem). Other related works include Jourdain and Zhou (2020); Lacker et al. (2019). In a recent work of Cuchiero et al. (2020), the LSV calibration problem was addressed from a deep learning point of view. In particular, the leverage function is parameterised by a class of feed-forward neural networks, and the model is calibrated by a generative adversarial network approach. In the present work, inspired by the theory of optimal transport, we introduce a variational approach for calibrating LSV models that does not require any form of interpolation.

In recent years, optimal transport theory has attracted the attention of many researchers. The problem was first addressed by Monge (1781) in the context of civil engineering and was later given a modern mathematical treatment by Kantorovich (1948). In 2000, in a landmark paper, Benamou and Brenier (2000) introduced a time-continuous formulation of the problem, which they solved numerically by an augmented Lagrangian method. In Brenier (1999) and Loeper (2006), the dual formulation of the time-continuous optimal transport has been formally expressed and generalised as an application of the Fenchel–Rockafellar theorem (see e.g., Villani, 2003, Theorem 1.9). This method has been also applied in Huesmann and Trevisan (2019) to study a time-continuous formulation of the martingale optimal transport. Recently, the problem has then been extended to transport by semi-martingales. Tan and Touzi (2013) studied the optimal transport problem for semi-martingales with constraints on the marginals at initial and final times. More recently, in Guo and Loeper (2018), the semi-martingale optimal transport problem was further extended to a more general path-dependent setting.

In the area of mathematical finance, optimal transport theory has recently been applied to many different problems, see e.g., Dolinsky and Soner (2014); Henry-Labordère and Touzi (2016); Pal et al. (2018). In terms of volatility model calibration by optimal transport, in the previous

work (Guo et al., 2019), the authors explored the idea of calibrating LV models to European options, in which they adapted the augmented Lagrangian method of Benamou and Brenier (2000) to one-dimensional martingale optimal transport. Later in Guo and Loeper (2018), the first two authors expanded the calibrating instruments from European options to path-dependent options, such as Asian options, barrier options and lookback options. We also mention that a variational calibration method of the LV model was proposed in Avellaneda et al. (1997) much earlier, although the connection with optimal transport was not established at that time. In addition to the LV models, a new class of SV models were developed, in Henry-Labordere (2019), inspired by the so-called Schrödinger bridge problem which is closely related to optimal transport. The calibration of these new SV models is achieved by modifying only the drift and leaving the volatility of volatility unchanged. Apart from continuous models, as an extension of March and Henry-Labordere (2019), Guyon (2020) constructed a discrete-time model which solves the challenging joint calibration problem of SPX and VIX options. Recently in Guo et al. (2020), we propose a continuous-time model to solve also the joint calibration problem by extending the approach of this paper.

In this paper, we further extend the approach of Guo et al. (2019) and Guo and Loeper (2018) to the calibration of LSV models. The calibration problem is formulated as a semi-martingale optimal transport problem. Unlike Tan and Touzi (2013), we consider a finite number of discrete constraints given by the prices of European claims. As a consequence of Jensen's inequality, we show that the optimal diffusion process is Markovian in the state variables given by the initial SV model. This result leads to a PDE formulation. By following the duality theory of optimal transport introduced in Brenier (1999) and a smoothing argument used in Bouchard et al. (2017), we establish a dual formulation. We also provide a numerical method to solve a fully non-linear Hamilton–Jacobi–Bellman (HJB) equation arising in the dual formulation. Finally, numerical examples show that the model can be fully calibrated to the European options with both simulated data and FX market data.

Despite its accuracy, our method is quite demanding in terms of computational power. The gradient descent demands at each step to solve one non-linear 2d PDE, and the computation of the gradient requires one (linear) 2d PDE per instrument. The most costly operation of numerically solving a linear PDE is inverting a large sparse matrix. However, this operation only needs to be carried once per time step because the computations of all components of the gradient are computed by solving the same linear PDE but with different terminal conditions. Alternatively, all gradients can be efficiently computed in one Monte Carlo simulation, which is a choice we did not make here for the sake of accuracy. Going into higher dimensions (a multifactor stochastic volatility model for example) would require to increase the dimension of the PDEs, which is problematic as soon as $d \geq 3$. When the goal is only to solve the usual LSV calibration problem, i.e., to find the leverage function, other methods achieve the result faster. For example, for a one-factor model, the PDE method of Ren et al. (2007) only requires solving a two-dimensional non-linear PDE once, and the particle method of Guyon and Henry-Labordere (2011) is even faster and can be applied to high dimensional cases (e.g., calibrating an LSV model with multiple stochastic factors). On the other hand, with the technique developed in this paper, one can fit path-dependent products (Guo and Loeper, 2018), SPX and VIX options (Guo et al., 2020) and here LSV models. Therefore the interest of our method is clearly its broad range of applications, at the cost of a relatively heavy computational cost. We also believe that with the recent developments of numerical methods for solving non-linear PDEs in high dimensions (see e.g., Han et al., 2020), our method can be greatly improved in terms of computational speed, and become applicable in high dimensions. Also notice that, being based on gradient descent, for a slight update of the market data, only a few gradient iterations should be needed to update the model. Finally, our method provides a rigorous existence result of an LSV type model. Previous works by Abergel and Tachet (2010) only provide an existence result for small times (see also Jourdain and Zhou (2020); Lacker et al. (2019)).

The paper is organised as follows: In Section 2, we introduce some preliminary definitions. In Section 3, we show the connection between the semi-martingale optimal transport problem and a PDE formulation. Duality results are then established for the PDE formulation. In Section 4, we demonstrate the calibration method using a Heston-like LSV model. Numerical method and results with both simulated data and FX market data are provided in Section 5.

2 Preliminaries

Given a Polish space E equipped with its Borel σ -algebra, let C(E) be the space of continuous functions on E and $C_b(E)$ be the space of bounded continuous functions. Denote by $\mathcal{M}(E)$ the space of finite signed Borel measures endowed with the weak-* topology. Let $\mathcal{M}_+(E) \subset \mathcal{M}(E)$ denote the subset of nonnegative measures. If E is compact, the topological dual of $C_b(E)$ is given by $C_b(E)^* = \mathcal{M}(E)$. More generally, if E is non-compact, $C_b(E)^*$ is larger than $\mathcal{M}(E)$. Let $\mathcal{P}(E)$ be the space of Borel probability measures, BV(E) be the space of functions of bounded variation and $L^1(d\mu)$ be the space of μ -integrable functions. We also write $C_b(E, \mathbb{R}^d)$, $\mathcal{M}(E, \mathbb{R}^d)$, $BV(E, \mathbb{R}^d)$ and $L^1(d\mu, \mathbb{R}^d)$ as the vector-valued versions of their corresponding spaces. Denote by \mathbb{S}^d the set of $d \times d$ symmetric matrices and $\mathbb{S}^d_+ \subset \mathbb{S}^d$ the set of positive semidefinite matrices. For any matrices $A, B \in \mathbb{S}^d$, we write $A : B := \operatorname{tr}(A^\intercal B)$ for their scalar product. For convenience, let $\Lambda = [0,T] \times \mathbb{R}^d$ and $\mathcal{X} = \mathbb{R} \times \mathbb{R}^d \times \mathbb{S}^d$. We use the notation $\langle \cdot, \cdot \rangle$ to denote the duality bracket between $C_b(\Lambda, \mathcal{X})$ and $C_b(\Lambda, \mathcal{X})^*$.

Let $\Omega := C([0,T],\mathbb{R}^d), T > 0$ be the canonical space with the canonical process X and the canonical filtration $\mathbb{F} = (\mathcal{F}_t)_{0 \le t \le T}$ generated by X. We denote by \mathcal{P} the collection of all probability measures \mathbb{P} on (Ω, \mathcal{F}_T) under which $X \in \Omega$ is an (\mathbb{F}, \mathbb{P}) -semi-martingale given by

$$X_t = X_0 + A_t + M_t, \quad t \in [0, T], \quad \mathbb{P}\text{-a.s.},$$

where M is an (\mathbb{F}, \mathbb{P}) -martingale with quadratic variation $\langle X_t \rangle = \langle M_t \rangle = B_t$, and the processes A and B are \mathbb{P} -a.s. absolutely continuous with respect to t. We say \mathbb{P} is *characterised* by $(\alpha^{\mathbb{P}}, \beta^{\mathbb{P}})$ if

$$\alpha_t^{\mathbb{P}} = \frac{dA_t^{\mathbb{P}}}{dt}, \quad \beta_t^{\mathbb{P}} = \frac{dB_t^{\mathbb{P}}}{dt},$$

where $(\alpha^{\mathbb{P}}, \beta^{\mathbb{P}})$ take values in the space $\mathbb{R}^d \times \mathbb{S}^d_+$. Note that $(\alpha^{\mathbb{P}}, \beta^{\mathbb{P}})$ is \mathbb{F} -adapted and determined up to $d\mathbb{P} \times dt$, almost everywhere. Let $\mathcal{P}^1 \subset \mathcal{P}$ be a subset of probability measures \mathbb{P} under which the characteristics $(\alpha^{\mathbb{P}}, \beta^{\mathbb{P}})$ are \mathbb{P} -integrable on the interval [0, T]. In other words,

$$\mathbb{E}^{\mathbb{P}}\left(\int_{0}^{T}|\alpha_{t}^{\mathbb{P}}|+|\beta_{t}^{\mathbb{P}}|\,dt\right)<+\infty,$$

where $|\cdot|$ is the L^1 -norm.

Given a vector $\tau := (\tau_1, \dots, \tau_m) \in (0, T]^m$, denote by G a vector of m functions such that each function $G_i \in C_b(\mathbb{R}^d)$ for $i = 1, \dots, m$. Given a Dirac measure $\mu_0 = \delta_{x_0}$ and a vector $c \in \mathbb{R}^m$, we define $\mathcal{P}(\mu_0, \tau, c, G) \subset \mathcal{P}^1$ as follows:

$$\mathcal{P}(\mu_0, \tau, c, G) := \{ \mathbb{P} : \mathbb{P} \in \mathcal{P}^1, \, \mathbb{P} \circ X_0^{-1} = \mu_0 \text{ and } \mathbb{E}^{\mathbb{P}}[G_i(X_{\tau_i})] = c_i, \, i = 1, \dots, m \}.$$

Assumption 2.1. The final time T coincides with the longest maturity, i.e., $T = \max_k \tau_k$.

For technical reasons, we restrict ourselves to functions G_i in $C_b(\mathbb{R}^d)$. In the context of volatility models calibration, G_i are discounted European payoffs. Although the call option payoff functions are not technically in $C_b(\mathbb{R}^d)$, we only work with them in a truncated (compact) space in practice. Alternatively, one may consider only put options using put-call parity.

3 Main results

3.1 Formulations

In this section, we first formulate the semi-martingale optimal transport problem under discrete constraints. Then a PDE formulation is introduced along with its dual counterpart.

Define the cost function $F: \Lambda \times \mathbb{R}^d \times \mathbb{S}^d \to \mathbb{R} \cup \{+\infty\}$ where $F(t, x, \alpha, \beta) = +\infty$ if $\beta \notin \mathbb{S}^d_+$, and $F(t, x, \alpha, \beta)$ is nonnegative, proper and lower semi-continuous in (α, β) . We also let F be strongly convex in (α, β) , i.e., there exists a constant C > 0 such that for all $t, x, \alpha, \beta, \alpha', \beta'$ and any subderivative ∇F , where ∇ is performed over (α, β) , if $F(t, x, \alpha, \beta)$ is finite then

$$F(t, x, \alpha', \beta') > F(t, x, \alpha, \beta) + \langle \nabla F(t, x, \alpha, \beta), (\alpha' - \alpha, \beta' - \beta) \rangle + C(\|\alpha' - \alpha\|^2 + \|\beta' - \beta\|^2),$$

where $\|\cdot\|$ denotes the Euclidean norm on \mathbb{R}^d and \mathbb{S}^d . Its convex conjugate $F^*: \Lambda \times \mathbb{R}^d \times \mathbb{S}^d \to \mathbb{R} \cup \{+\infty\}$ for (α, β) is then defined as

$$F^*(t,x,a,b) := \sup_{\alpha \in \mathbb{R}^d, \beta \in S^d_+} \left\{ \alpha \cdot a + \beta : b - F(t,x,\alpha,\beta) \right\}.$$

For simplicity, we write $F(\alpha, \beta) := F(t, x, \alpha, \beta)$ and $F^*(a, b) := F^*(t, x, a, b)$ if there is no ambiguity. Note that our definition of strongly convex does not require F to be differentiable, since only subderivatives are used. Nevertheless, it implies that F is strictly convex and thus F^* is differentiable.

Adopting the convention inf $\emptyset = +\infty$, we are interested in the following minimisation problem:

Problem 1. Given μ_0, τ, c and G, we want to find

$$\mathcal{V} = \inf_{\mathbb{P} \in \mathcal{P}(\mu_0, \tau, c, G)} \mathbb{E}^{\mathbb{P}} \int_0^T F(\alpha_t^{\mathbb{P}}, \beta_t^{\mathbb{P}}) dt.$$

The problem is said to be admissible if $\mathcal{P}(\mu_0, \tau, c, G)$ is nonempty and the infimum above is finite.

It is well known that the marginal distributions of diffusion processes at fixed times solve the Fokker–Planck equation in the weak sense. The converse result was given by Figalli (2008) and

Trevisan (2016). For brevity, we write $\mathbb{E}_{t,x}^{\mathbb{P}} := \mathbb{E}^{\mathbb{P}}[\cdot \mid X_t = x]$. As an immediate consequence of Itô's formula and Theorem 2.5 in Trevisan (2016), we introduce the following lemma.

Lemma 3.1. Let $\mathbb{P} \in \mathcal{P}^1$ and $\rho_t^{\mathbb{P}} = \rho^{\mathbb{P}}(t, \cdot) = \mathbb{P} \circ X_t^{-1}$ be the marginal distribution of X_t under \mathbb{P} , $t \leq T$. Then $\rho^{\mathbb{P}}$ is a weak solution to the Fokker–Planck equation:

$$\begin{cases}
\partial_t \rho_t^{\mathbb{P}} + \nabla_x \cdot (\rho_t^{\mathbb{P}} \mathbb{E}_{t,x}^{\mathbb{P}} \alpha_t^{\mathbb{P}}) - \frac{1}{2} \sum_{i,j} \partial_{ij} (\rho_t^{\mathbb{P}} (\mathbb{E}_{t,x}^{\mathbb{P}} \beta_t^{\mathbb{P}})_{ij}) = 0 & in [0,T] \times \mathbb{R}^2, \\
\rho_0^{\mathbb{P}} = \delta_{X_0} & in \mathbb{R}^2.
\end{cases} \tag{1}$$

Moreover, there exists another probability measure $\mathbb{P}' \in \mathcal{P}^1$ under which X has the same marginals, $\rho^{\mathbb{P}'} = \rho^{\mathbb{P}}$, and is a Markov process solving

$$\begin{cases}
 dX_t = \alpha^{\mathbb{P}'}(t, X_t) dt + (\beta^{\mathbb{P}'}(t, X_t))^{\frac{1}{2}} dW_t^{\mathbb{P}'}, & 0 \le t \le T, \\
 X_0 = x_0,
\end{cases}$$
(2)

where $W^{\mathbb{P}'}$ is a \mathbb{P}' -Brownian motion, $\alpha^{\mathbb{P}'}(t,X_t) = \mathbb{E}_{t,X_t}^{\mathbb{P}} \alpha_t^{\mathbb{P}}$ and $\beta^{\mathbb{P}'}(t,X_t) = \mathbb{E}_{t,X_t}^{\mathbb{P}} \beta_t^{\mathbb{P}}$.

The above lemma provides a solution to study semi-martingales via Markov processes in the form of (2). It is worth noting that the idea of using diffusion processes to mimic an Itô process by matching their marginals at fixed times traces back to the classical mimicking theorem of Gyöngy (1986), which was significantly extended later by Brunick and Shreve (2013). In fact, Lemma 3.1 can be seen as a reformulation of Brunick and Shreve (2013, Corollary 3.7) which was constructed by a completely different approach. The Markov processes X in (2) are also called Markovian projections in the literature.

Definition 3.2. Define $\mathcal{P}_{loc}(\mu_0, \tau, c, G)$ to be a subset of $\mathcal{P}(\mu_0, \tau, c, G)$ such that, under any $\mathbb{P} \in \mathcal{P}_{loc}(\mu_0, \tau, c, G)$, X is a Markov process that takes the form of (2), and X has an initial marginal μ_0 and satisfies $\mathbb{E}^{\mathbb{P}}[G_i(X_{\tau_i})] = c_i$ for all i = 1, ..., m.

Lemma 3.3. If $\mathcal{P}(\mu_0, \tau, c, G)$ is not empty, then $\mathcal{P}_{loc}(\mu_0, \tau, c, G)$ is not empty. Moreover, for any $\mathbb{P} \in \mathcal{P}(\mu_0, \tau, c, G)$, there exists a $\mathbb{P}' \in \mathcal{P}_{loc}(\mu_0, \tau, c, G)$ such that X has the same marginals under \mathbb{P} and \mathbb{P}' .

Proof. Assume that $\mathcal{P}(\mu_0, \tau, c, G)$ is not empty, for any $\mathbb{P} \in \mathcal{P}(\mu_0, \tau, c, G)$, by Lemma 3.1, exists $\mathbb{P}' \in \mathcal{P}^1$ such that X is a Markov process that has the same marginals $\rho^{\mathbb{P}'} = \rho^{\mathbb{P}}$ and takes the form of (2) with coefficients $(\alpha^{\mathbb{P}'}(t, X_t), \beta^{\mathbb{P}'}(t, X_t)) = (\mathbb{E}^{\mathbb{P}}_{t, X_t} \alpha^{\mathbb{P}}_t, \mathbb{E}^{\mathbb{P}}_{t, X_t} \beta^{\mathbb{P}}_t)$. Since $\rho^{\mathbb{P}'} = \rho^{\mathbb{P}}$, X has the initial marginal μ_0 and satisfies $\mathbb{E}^{\mathbb{P}'}[G_i(X_{\tau_i})] = c_i$ for all $i = 1, \ldots, m$ under both \mathbb{P} and \mathbb{P}' . Thus, $\mathbb{P}' \in \mathcal{P}_{loc}(\mu_0, \tau, c, G)$.

Applying Lemma 3.3 and taking advantage of the convexity of the cost function, we establish the following result:

Proposition 3.4. Given μ_0, τ, c and G, then

$$\mathcal{V} = \inf_{\mathbb{P} \in \mathcal{P}(\mu_0, \tau, c, G)} \mathbb{E}^{\mathbb{P}} \int_0^T F(\alpha_t^{\mathbb{P}}, \beta_t^{\mathbb{P}}) dt = \inf_{\mathbb{P} \in \mathcal{P}_{loc}(\mu_0, \tau, c, G)} \mathbb{E}^{\mathbb{P}} \int_0^T F(\alpha^{\mathbb{P}}(t, X_t), \beta^{\mathbb{P}}(t, X_t)) dt.$$
 (3)

Proof. If $\mathcal{P}(\mu_0, \tau, c, G)$ is empty, then $\mathcal{P}_{loc}(\mu_0, \tau, c, G)$ is empty since $\mathcal{P}_{loc}(\mu_0, \tau, c, G) \subset \mathcal{P}(\mu_0, \tau, c, G)$. Thus, (3) holds and $\mathcal{V} = +\infty$. If $\mathcal{P}(\mu_0, \tau, c, G)$ is not empty, by Lemma 3.3, $\mathcal{P}_{loc}(\mu_0, \tau, c, G)$ is not empty. For any $\mathbb{P} \in \mathcal{P}(\mu_0, \tau, c, G)$, let $\mathbb{P}' \in \mathcal{P}_{loc}(\mu_0, \tau, c, G)$ be the probability measure such that X has the same marginals under \mathbb{P} and \mathbb{P}' . Applying Jensen's inequality together with the tower property of conditional expectation, we have

$$\mathbb{E}^{\mathbb{P}} \int_{0}^{T} F(\alpha_{t}^{\mathbb{P}}, \beta_{t}^{\mathbb{P}}) dt = \mathbb{E}^{\mathbb{P}} \int_{0}^{T} \mathbb{E}_{t, X_{t}}^{\mathbb{P}} F(\alpha_{t}^{\mathbb{P}}, \beta_{t}^{\mathbb{P}}) dt$$

$$\geq \mathbb{E}^{\mathbb{P}} \int_{0}^{T} F(\mathbb{E}_{t, X_{t}}^{\mathbb{P}} \alpha_{t}^{\mathbb{P}}, \mathbb{E}_{t, X_{t}}^{\mathbb{P}} \beta_{t}^{\mathbb{P}}) dt$$

$$= \mathbb{E}^{\mathbb{P}'} \int_{0}^{T} F(\alpha^{\mathbb{P}'}(t, X_{t}), \beta^{\mathbb{P}'}(t, X_{t})) dt.$$

$$(4)$$

The last $\mathbb{E}^{\mathbb{P}}$ is replaced by $\mathbb{E}^{\mathbb{P}'}$ because the marginal of X is the same under \mathbb{P} and \mathbb{P}' . Since $\mathcal{P}_{loc}(\mu_0, \tau, c, G) \subset \mathcal{P}(\mu_0, \tau, c, G)$, taking infimum over all $\mathbb{P} \in \mathcal{P}(\mu_0, \tau, c, G)$ on the left-hand side and over all $\mathbb{P}' \in \mathcal{P}_{loc}(\mu_0, \tau, c, G)$ on the right-hand side of (4), we obtain the required result. \square

Proposition 3.4 shows that it suffices to consider only the probability measures in $\mathcal{P}_{loc}(\mu_0, \tau, c, G)$. Thus, by the connections established in Lemma 3.1, Problem 1 can be studied via PDE methods. Following the Benamou–Brenier formulation of the classical optimal transport from Benamou and Brenier (2000), we introduce the following problem:

Problem 2 (PDE formulation). Given μ_0, τ, c and G, we want to minimise

$$\mathcal{V} = \inf_{\rho,\alpha,\beta} \int_0^T \int_{\mathbb{R}^d} F(\alpha(t,x),\beta(t,x)) \, d\rho(t,x) dt, \tag{5}$$

among all $(\rho, \alpha, \beta) \in C([0, T], \mathcal{P}(\mathbb{R}^d) - w*) \times L^1(d\rho_t dt, \mathbb{R}^d) \times L^1(d\rho_t dt, \mathbb{S}^d)$ satisfying (in the distributional sense)

$$\partial_t \rho(t, x) + \nabla_x \cdot (\rho(t, x)\alpha(t, x)) - \frac{1}{2} \sum_{i,j} \partial_{ij} (\rho(t, x)\beta_{ij}(t, x)) = 0, \tag{6}$$

$$\int_{\mathbb{R}^d} G_i(x) \, d\rho(\tau_i, x) = c_i, \ \forall i = 1, \dots, m, \qquad \text{and} \qquad \rho(0, \cdot) = \mu_0. \tag{7}$$

The interchange of integrals in (5) is justified by Fubini's theorem as F is nonnegative. For the weak continuity of measure ρ in time, the reader can refer to Loeper (2006, Theorem 3).

Before ending this section, based on the results of Sections 3.2 and 3.3 below, we shall introduce a dual formulation of Problem 2. The definition of the viscosity solution to (9) and the proof will be given in Section 3.3.

Proposition 3.5 (Dual formulation). Given μ_0, τ, c and G,

$$\mathcal{V} = \sup_{\lambda \in \mathbb{R}^m} \sum_{i=1}^m \lambda_i c_i - \int_{\mathbb{R}^d} \phi(0, x) \, d\mu_0, \tag{8}$$

where ϕ is the viscosity solution to the HJB equation

$$\partial_t \phi + \sum_{i=1}^m \lambda_i G_i \delta_{\tau_i} + F^*(\nabla_x \phi, \frac{1}{2} \nabla_x^2 \phi) = 0, \quad in [0, T) \times \mathbb{R}^d,$$
(9)

with the terminal condition $\phi(T,\cdot)=0$. Moreover, if \mathcal{V} is finite, then the infimum of Problem 2 is attained. If the supremum is attained by some λ for which the associated solution to (9) is $\phi^* \in BV([0,T], C_b^2(\mathbb{R}^d))$, and if (ρ, α, β) is an optimal solution of Problem 2, then (α, β) is given by

$$(\alpha_t, \beta_t) = \nabla F^*(\nabla_x \phi^*(t, \cdot), \frac{1}{2} \nabla_x^2 \phi^*(t, \cdot)), \quad d\rho_t dt - almost \ everywhere. \tag{10}$$

3.2 Duality

This section is devoted to establish the duality by closely following Loeper (2006, Section 3.2) (see also Brenier, 1999; Huesmann and Trevisan, 2019).

Theorem 3.6. Given μ_0, τ, c and G,

$$\mathcal{V} = \sup_{\phi, \lambda} \sum_{i=1}^{m} \lambda_i c_i - \int_{\mathbb{R}^d} \phi(0, x) \, d\mu_0, \tag{11}$$

where the supremum is taken over all $(\phi, \lambda) \in BV([0, T], C_b^2(\mathbb{R}^d)) \times \mathbb{R}^m$ satisfying

$$\partial_t \phi + \sum_{i=1}^m \lambda_i G_i \delta_{\tau_i} + F^*(\nabla_x \phi, \frac{1}{2} \nabla_x^2 \phi) \le 0 \qquad in [0, T) \times \mathbb{R}^d, \tag{12}$$

and $\phi(T,\cdot)=0$. Moreover, if \mathcal{V} is finite, then the infimum of Problem 2 is attained.

Proof. The proof relies on the Fenchel–Rockafellar theorem which plays a key role in the applications of convex analysis. One may note that the objective function (5) is not convex in (ρ, α, β) . Define measures $\mathcal{A} := \rho \alpha$ and $\mathcal{B} := \rho \beta$, then \mathcal{A} and \mathcal{B} are absolutely continuous with respect to ρ . By identifying the parameterisation by $(\rho, \mathcal{A}, \mathcal{B})$, the objective function (5) is convex in $(\rho, \mathcal{A}, \mathcal{B})$. In addition, the constraints (6) and (7) are linear in $(\rho, \mathcal{A}, \mathcal{B})$.

The constraints (6) and (7) can be formulated in the following weak form:

$$\forall \phi \in C_c^{\infty}(\Lambda), \qquad \int_{\Lambda} \partial_t \phi \, d\rho + \nabla_x \phi \cdot d\mathcal{A} + \frac{1}{2} \nabla_x^2 \phi : d\mathcal{B} + \int_{\mathbb{P}^d} \phi(0, \cdot) \, d\mu_0 = 0, \qquad (13)$$

$$\forall \lambda \in \mathbb{R}^m, \qquad \int_{\Lambda} \sum_{i=1}^m \lambda_i G_i \delta_{\tau_i} d\rho - \sum_{i=1}^m \lambda_i c_i = 0.$$
 (14)

Thus Problem 2 can be reformulated as the following saddle point problem:

$$\mathcal{V} = \inf_{\rho, \mathcal{A}, \mathcal{B}} \sup_{\phi, \lambda} \left\{ \int_{\Lambda} F\left(\frac{d\mathcal{A}}{d\rho}, \frac{d\mathcal{B}}{d\rho}\right) d\rho - \partial_{t}\phi d\rho - \nabla_{x}\phi \cdot d\mathcal{A} - \frac{1}{2}\nabla_{x}^{2}\phi : d\mathcal{B} - \int_{\mathbb{R}^{d}} \phi(0, \cdot) d\mu_{0} \right. \\
\left. - \int_{\Lambda} \sum_{i=1}^{m} \lambda_{i} G_{i} \delta_{\tau_{i}} d\rho + \sum_{i=1}^{m} \lambda_{i} c_{i} \right\}.$$
(15)

The strategy of the proof is to first construct a function Φ whose convex conjugate Φ^* is equal to the objective function of Problem 2, and construct another function Ψ whose convex conjugate Ψ^* is equal to the rest part inside the infimum of (15) so that $\mathcal{V} = \inf_{\rho, \mathcal{A}, \mathcal{B}} (\Phi^* + \Psi^*)(\rho, \mathcal{A}, \mathcal{B})$. Then, the duality is established by applying the Fenchel–Rockafellar theorem.

Adopting the terminology of Huesmann and Trevisan (2019), we say the triple (r, a, b) is rep-

resented by (ϕ, λ) if it satisfies

$$r + \partial_t \phi + \sum_{i=1}^m \lambda_i G_i \delta_{\tau_i} = 0,$$
$$a + \nabla_x \phi = 0,$$
$$b + \frac{1}{2} \nabla_x^2 \phi = 0.$$

If we choose (r, a, b) from $C_b(\Lambda, \mathcal{X})$, then ϕ has possible jump discontinuities at $t = \tau_i$ due to the presence of the Dirac delta functions. Now, define functionals $\Phi : C_b(\Lambda, \mathcal{X}) \to \mathbb{R} \cup \{+\infty\}$ and $\Psi : C_b(\Lambda, \mathcal{X}) \to \mathbb{R} \cup \{+\infty\}$ as follows:

$$\Phi(r,a,b) = \begin{cases} 0 & \text{if } r + F^*(a,b) \leq 0, \\ +\infty & \text{otherwise,} \end{cases}$$

$$\Psi(r,a,b) = \begin{cases} \int_{\mathbb{R}^d} \phi(0,x) \, d\mu_0 - \sum_{i=1}^m \lambda_i c_i & \text{if } (r,a,b) \text{ is represented by} \\ (\phi,\lambda) \in BV([0,T], C_b^2(\mathbb{R}^d)) \times \mathbb{R}^m, \\ +\infty & \text{otherwise.} \end{cases}$$

Denote by Φ^* and Ψ^* the convex conjugates of Φ and Ψ , respectively. For Φ , its convex conjugate $\Phi^*: C_b(\Lambda, \mathcal{X})^* \to \mathbb{R} \cup \{+\infty\}$ is given by

$$\Phi^*(\rho, \mathcal{A}, \mathcal{B}) = \sup_{(r, a, b) \in C_b(\Lambda, \mathcal{X})} \{ \langle (r, a, b), (\rho, \mathcal{A}, \mathcal{B}) \rangle \; ; \; r + F^*(a, b) \le 0 \}.$$

As shown in Lemma A.1, if we restrict Φ^* to $\mathcal{M}(\Lambda, \mathcal{X})$, then

$$\Phi^*(\rho, \mathcal{A}, \mathcal{B}) = \begin{cases} \int_{\Lambda} F\left(\frac{d\mathcal{A}}{d\rho}, \frac{d\mathcal{B}}{d\rho}\right) d\rho & \text{if } \rho \in \mathcal{M}_+(\Lambda, \mathcal{X}) \text{ and } (\mathcal{A}, \mathcal{B}) \ll \rho, \\ +\infty & \text{otherwise.} \end{cases}$$

Next, $\Psi^*: C_b(\Lambda, \mathcal{X})^* \to \mathbb{R} \cup \{+\infty\}$ is given by

$$\Psi^*(\rho, \mathcal{A}, \mathcal{B}) = \sup_{r, a, b} \langle (r, a, b), (\rho, \mathcal{A}, \mathcal{B}) \rangle - \int_{\mathbb{R}^d} \phi(0, x) \, d\mu_0 + \sum_{i=1}^m \lambda_i c_i,$$

where the supremum is taken over all triples $(r, a, b) \in C_b(\Lambda, \mathcal{X})$ represented by (ϕ, λ) in $BV([0, T], C_b^2(\mathbb{R}^d)) \times \mathbb{R}^m$. In terms of (ϕ, λ) ,

$$\Psi^*(\rho, \mathcal{A}, \mathcal{B}) = \sup_{\phi, \lambda} \langle (-\partial_t \phi - \sum_{i=1}^m \lambda_i G_i \delta_{\tau_i}, -\nabla_x \phi, -\frac{1}{2} \nabla_x^2 \phi), (\rho, \mathcal{A}, \mathcal{B}) \rangle - \int_{\mathbb{R}^d} \phi(0, x) \, d\mu_0 + \sum_{i=1}^m \lambda_i c_i.$$

As proved in Lemma A.2, the objective V can be expressed as

$$\mathcal{V} = \inf_{(\rho, \mathcal{A}, \mathcal{B}) \in \mathcal{M}(\Lambda, \mathcal{X})} (\Phi^* + \Psi^*)(\rho, \mathcal{A}, \mathcal{B}) = \inf_{(\rho, \mathcal{A}, \mathcal{B}) \in C_b(\Lambda, \mathcal{X})^*} (\Phi^* + \Psi^*)(\rho, \mathcal{A}, \mathcal{B}).$$

Let $O^{m \times n}$ denote a null matrix of size $m \times n$. Consider the point $(r, a, b) = (-1, O^{d \times 1}, O^{d \times d})$ which can be represented by $(\phi, \lambda) = (-t, O^{m \times 1})$. As F is nonnegative, at $(-1, O^{d \times 1}, O^{d \times d})$ we

have

$$-1 + F^*(O^{d \times 1}, O^{d \times d}) = -1 - \inf_{\alpha \in \mathbb{R}^d, \beta \in \mathbb{S}^d} F(\alpha, \beta) < 0.$$

This shows that

$$\Phi(-1, O^{d \times 1}, O^{d \times d}) = 0, \quad \Psi(-1, O^{d \times 1}, O^{d \times d}) = 0.$$

Thus, at $(-1, O^{d \times 1}, O^{d \times d})$, Φ is continuous with respect to the uniform norm (since F^* is continuous in $\text{dom}(F^*)$), and Ψ is finite. Furthermore, as the convex functionals Φ and Ψ take values in $(-\infty, +\infty]$, all of the required conditions are fulfilled to apply the Fenchel–Rockafellar duality theorem (see e.g., Brezis, 2011, Chapter 1). We then obtain

$$\mathcal{V} = \inf_{(\rho, \mathcal{A}, \mathcal{B}) \in C_b(\Lambda, \mathcal{X})^*} \{ \Phi^*(\rho, \mathcal{A}, \mathcal{B}) + \Psi^*(\rho, \mathcal{A}, \mathcal{B}) \} = \sup_{(r, a, b) \in C_b(\Lambda, \mathcal{X})} \{ -\Phi(-r, -a, -b) - \Psi(r, a, b) \},$$

and the infimum is in fact attained. Consequently,

$$\mathcal{V} = \sup_{r,a,b} \left\{ -\int_{\mathbb{R}^d} \phi(0,x) \, d\mu_0 + \sum_{i=1}^m \lambda_i c_i \; ; \; -r + F^*(-a,-b) \le 0 \right\},\,$$

where the supremum is restricted to all (r, a, b) represented by $(\phi, \lambda) \in BV([0, T], C_b^2(\mathbb{R}^d)) \times \mathbb{R}^m$. Writing (r, a, b) in terms of (ϕ, λ) and fixing $\phi(t = T) = 0$, we obtain the required result.

3.3 Viscosity solutions

Adopting the concept of viscosity solutions, it can be shown that the supremum of the objective with respect to ϕ is achieved by the viscosity solution the HJB equation (9). Due to presence of the Dirac delta functions in (9), we shall introduce a suitable definition of the viscosity solution that allows to have jump discontinuities in time.

Definition 3.7. Denote by $set(\tau)$ the set of entries of vector τ and by K the cardinality of $set(\tau)$. Let $t_0 = 0$, we define disjoint intervals $I_k := [t_{k-1}, t_k)$ such that

$$\bigcup_{k=1}^{K} I_k = [0, T),$$

where $t_{k-1} < t_k$ and $t_k \in set(\tau)$ for all k = 1, ..., K.

Definition 3.8 (Viscosity solution). For any $\lambda \in \mathbb{R}^m$, we say ϕ is a viscosity subsolution (resp., supersolution) of (9) if ϕ is a classical (continuous) viscosity subsolution (resp., supersolution) of (9) in $I_k \times \mathbb{R}^d$ for all k = 1, ..., K, and has jump discontinuities:

$$\phi(t,x) = \phi(t^-,x) - \sum_{i=1}^m \lambda_i G_i(x) \mathbb{1}(t=\tau_i) \qquad \forall (t,x) \in \tau \times \mathbb{R}^d.$$

Then, ϕ is called a viscosity solution of (9) if ϕ is both a viscosity subsolution and a viscosity supersolution of (9).

Remark 3.9 (Comparison principle). The comparison principle still holds for viscosity solutions of (9). Let u and v be a viscosity subsolution and a viscosity supersolution of the equation (9), respectively. At the terminal time T, $u(T,\cdot) \leq v(T,\cdot)$. Since $t_K = T$ is in $\operatorname{set}(\tau)$ and u,v have the same jump size at $\{T\} \times \mathbb{R}^d$, we get $u(T^-,\cdot) \leq v(T^-,\cdot)$. Next, in the interval $I_K = [t_{K-1},t_K)$, by the classical comparison principle, we get $u \leq v$ on I_K . Applying this argument for all intervals I_k for $k = 1, \ldots, K$, we conclude that

$$u(t,x) \le v(t,x), \quad \forall (t,x) \in [0,T] \times \mathbb{R}^d.$$

Also, $u(0,\cdot) \le v(0,\cdot)$.

Remark 3.10 (Existence and uniqueness). As a consequence of the comparison principle, there exists a unique viscosity solution of (9). The uniqueness is a direct consequence of the comparison principle. The existence can be obtained by the Perron's method (see Crandall et al., 1992) under which the comparison principle is a key argument.

Now we shall prove Proposition 3.5. The proof relies on a smoothing argument used in Bouchard et al. (2017), which is based on the shaken coefficients technique of Krylov (2000). The proof is similar to Theorem 2.4 in Bouchard et al. (2017), which we sketch here for completeness.

Proof of Proposition 3.5. Denote by φ a viscosity solution of the equation (9) with any $\lambda \in \mathbb{R}^m$. From Remark 3.10, we know that such φ exists and is unique. The first part of the proposition is proved in two steps:

Step 1. Assuming that there exists a sequence of supersolutions of (9) in $BV([0,T], C_b^2(\mathbb{R}^d))$ converging to φ pointwise, we can show that φ achieves the supremum with respect to φ in the objective of the dual (11). Let $\varphi \in BV([0,T], C_b^2(\mathbb{R}^d))$ be any solution satisfies (12), and φ is also a (viscosity) supersolution of (9). By Remark 3.9, we have $\varphi(0,x) \leq \varphi(0,x)$ for all $x \in \mathbb{R}^d$, hence

$$\sum_{i=1}^{m} \lambda_i c_i - \int_{\mathbb{R}^d} \phi(0, x) \, d\mu_0 \le \sum_{i=1}^{m} \lambda_i c_i - \int_{\mathbb{R}^d} \varphi(0, x) \, d\mu_0.$$
 (16)

The equality can be achieved in (16) by taking the supremum with respect to ϕ on the left-hand side of (16).

Step 2. Now, we shall construct the sequence of supersolutions required in Step 1. Let us introduce the regularising kernel $r_{\varepsilon}: \mathbb{R}^d \to \mathbb{R}$ such that $r_{\varepsilon}(x) = \frac{1}{\varepsilon^d} r'\left(\frac{x}{\varepsilon}\right)$ where r' is some compactly supported function that satisfies $\int_{\mathbb{R}^d} r'(x) \, dx = 1$. Then we define $\varphi_{\varepsilon} = \varphi * r_{\varepsilon}$ where the convolution acts on only the variable x. By applying the result of Bouchard et al. (2017) which relies critically on the fact that $F^*(a,b)$ is convex in (a,b), it can be shown that φ_{ε} are supersolutions of equation (9). If we send ε to 0, the supersolutions φ_{ε} converges to the viscosity solution φ pointwise. The desired sequence is then constructed.

Now we prove the second part of the proposition. Let $(\rho^*, \alpha^*, \beta^*)$ be the optimal solution of Problem 2, then $(\rho^*, \rho^*\alpha^*, \rho^*\beta^*)$ also achieves the infimum (15). Assume that there exists an optimal solution λ^* that solves (8) and the associated solution to (9) is $\phi^* \in BV([0,T], C_b^2(\mathbb{R}^d))$, then (ϕ^*, λ^*) also achieve the supremum in (15). With the optimal solutions defined above, we

can reformulate (15) as

$$0 = \int_0^T \int_{\mathbb{R}^d} \left(F(\alpha^*, \beta^*) - \partial_t \phi^* - \nabla_x \phi^* \cdot \alpha^* - \frac{1}{2} \nabla_x^2 \phi^* : \beta^* - \sum_{i=1}^m \lambda_i^* G_i \delta_{\tau_i} \right) d\rho_t^* dt$$
$$= \int_0^T \int_{\mathbb{R}^d} \left(F(\alpha^*, \beta^*) + F^* \left(\nabla_x \phi^*, \frac{1}{2} \nabla_x^2 \phi^* \right) - \nabla_x \phi^* \cdot \alpha^* - \frac{1}{2} \nabla_x^2 \phi^* : \beta^* \right) d\rho_t^* dt.$$

Let $(\tilde{\alpha}, \tilde{\beta})$ be defined by

$$(\tilde{\alpha}, \tilde{\beta}) = \nabla F^* \left(\nabla_x \phi^*, \frac{1}{2} \nabla_x^2 \phi^* \right), \quad \left(\nabla_x \phi^*, \frac{1}{2} \nabla_x^2 \phi^* \right) = \nabla F(\tilde{\alpha}, \tilde{\beta}).$$

Hence, by the definition of convex conjugate and the strong convexity of F,

$$0 = \int_0^T \int_{\mathbb{R}^d} \left(F(\alpha^*, \beta^*) - F(\tilde{\alpha}, \tilde{\beta}) - \nabla_x \phi^* \cdot (\alpha^* - \tilde{\alpha}) - \frac{1}{2} \nabla_x^2 \phi^* : (\beta^* - \tilde{\beta}) \right) d\rho_t^* dt$$

$$\geq \int_0^T \int_{\mathbb{R}^d} C\left(\|\alpha^* - \tilde{\alpha}\|^2 + \|\beta^* - \tilde{\beta}\|^2 \right) d\rho_t^* dt \geq 0,$$

where C > 0 is a constant. Therefore, $(\alpha^*, \beta^*) = (\tilde{\alpha}, \tilde{\beta}), d\rho_t^* dt$ -almost everywhere. The proof is completed.

4 LSV Calibration

In this section, we illustrate our method by calibrating a Heston-like LSV model. This method could also be easily extended to other LSV models. We consider the LSV model with following dynamics under the risk-neutral measure:

$$\begin{cases}
 dZ_t = (r(t) - q(t) - \frac{1}{2}\sigma^2(t, Z_t, V_t)) dt + \sigma(t, Z_t, V_t) dW_t^Z, \\
 dV_t = \kappa(\theta - V_t) dt + \xi \sqrt{V_t} dW_t^V, \\
 dW_t^Z dW_t^V = \eta(t, Z_t, V_t) dt,
\end{cases}$$
(17)

where Z_t is the logarithm of the stock price at time t. The interpretations of r and q differ between financial markets. In the equity market, r is the risk-free rate and q is the dividend yield. In the FX market, r is the domestic interest rate and q is the foreign interest rate. The parameters κ, θ, ξ have the same interpretation as in the Heston model. In our method, we assume these parameters are given and obtained by calibrating a pure Heston model. Note that in the literature, the widely considered LSV model has a volatility function $\sigma(t, Z_t, V_t) = L(t, Z_t)\sqrt{V_t}$ and a constant correlation η , where $L(t, Z_t)$ is known as the leverage function. By contrast, we consider a local-stochastic volatility $\sigma > 0$ and a local-stochastic correlation $\eta \in [-1,1]$ whose values depend on (t, Z_t, V_t) . Our objective is to calibrate $\sigma(t, Z, V)$ and $\eta(t, Z, V)$ so that model prices exactly match market prices.

Remark 4.1. If the volatility $\sigma(t, Z, V) \equiv \sqrt{V}$ and the correlation $\eta(t, Z, V)$ is a constant, the LSV model reduces to a pure Heston model. Furthermore, if $\sigma(t, Z, V)$ is independent of the variable V, the model is equivalent to a local volatility model.

Consider a probability measure $\mathbb{P} \in \mathcal{P}^1$ and a two-dimensional \mathbb{P} -semi-martingale X_t . The

process X_t has dynamics (17), i.e., $X_t = (Z_t, V_t)$, if \mathbb{P} is characterised by $(\alpha^{\mathbb{P}}, \beta^{\mathbb{P}})$ such that

$$(\alpha_t^{\mathbb{P}}, \beta_t^{\mathbb{P}}) = \left(\begin{bmatrix} r_t - q_t - \frac{1}{2}\sigma_t^2 \\ \kappa(\theta - V_t) \end{bmatrix}, \begin{bmatrix} \sigma_t^2 & \eta_t \xi \sqrt{V_t} \sigma_t \\ \eta_t \xi \sqrt{V_t} \sigma_t & \xi^2 V_t \end{bmatrix} \right), \quad t \in [0, T], \tag{18}$$

with functions $\sigma_t = \sigma(t, Z_t, V_t)$ and $\eta_t = \eta(t, Z_t, V_t)$. Recall that the parameters (κ, θ, ξ) are assumed to be given. Also, r_t and q_t are known and V_t is the state variable. Hence, the only unknown variables in (18) are σ_t and η_t . As we will see below, σ_t will be the only free variable in the calibration. Given m European options with prices $c \in \mathbb{R}_+^m$, maturities $\tau = (\tau_1, \ldots, \tau_m) \in (0, T]^m$ and discounted payoffs $G = (G_1, \ldots, G_m)$ where $G_i : \mathbb{R}^d \to \mathbb{R}_+$ (e.g., $G_i(X) = e^{-\int_0^{\tau_i} r(s) ds} (e^{X_1} - K)^+$ for a European call with strike K and maturity τ_i). If X_t has an initial distribution $\mu_0 = \delta_{(Z_0, V_0)}$ and is exactly calibrated to the these European options, then $\mathbb{P} \in \mathcal{P}(\mu_0, \tau, c, G)$. The LSV calibration problem can be formulated as

$$\mathcal{V} = \inf_{\mathbb{P} \in \mathcal{P}(\mu_0, \tau, c, G)} \mathbb{E}^{\mathbb{P}} \int_0^T F(t, X_t, \alpha_t^{\mathbb{P}}, \beta_t^{\mathbb{P}}) dt, \tag{19}$$

where F is a suitable convex cost function that forces $(\alpha^{\mathbb{P}}, \beta^{\mathbb{P}})$ to take the form of (18).

One possible way to choose the cost function F is based on the idea of minimising the difference between each element of $\beta^{\mathbb{P}}$ and a reference value while keeping $\beta^{\mathbb{P}}$ in \mathbb{S}^2_+ . However, it is often impossible to find an explicit formula to approximate F^* . Thus numerical optimisation is needed, which makes the method computationally expensive. To overcome this issue, we choose the correlation

$$\eta_t = \frac{\sqrt{V_t}}{\sigma_t} \bar{\eta}, \quad t \in [0, T], \tag{20}$$

where $\bar{\eta}$ is a constant correlation obtained (along with κ, θ, ξ) by calibrating a pure Heston model. In this case, $\beta_t^{\mathbb{P}}$ is positive semidefinite if and only if $\sigma_t^2 \geq \bar{\eta}^2 V_t$ for $t \geq T$.

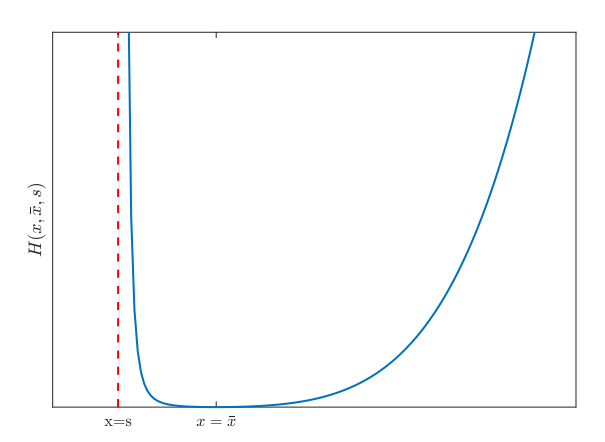


Figure 1: The function $H(x, \bar{x}, s)$ for a given \bar{x} and a given $s < \bar{x}$.

Definition 4.2. Define function $H: \mathbb{R} \times \mathbb{R}_+ \times \mathbb{R} \to \mathbb{R} \cup \{+\infty\}$ such that

$$H(x, \bar{x}, s) := \begin{cases} a(\frac{x-s}{\bar{x}-s})^{1+p} + b(\frac{x-s}{\bar{x}-s})^{1-p} + c & \text{if } x > s \text{ and } \bar{x} > s, \\ +\infty & \text{otherwise.} \end{cases}$$

The parameter p is a constant greater than 1, and a, b, c are constants determined to minimise the function at $x = \bar{x}$ with min H = 0.

Given \bar{x} and s satisfying $\bar{x} > s$, the function H is convex in x and minimised at \bar{x} . It is finite only when x > s. In the numerical examples (see Section 5.2 and 5.3 below), the parameter p is set to 4. A plot of H is given in Figure 1. Then, we define the cost function as follows.

Definition 4.3. The cost function $F: \mathbb{R} \times \mathbb{R} \times \mathbb{R} \times \mathbb{R}^2 \times \mathbb{S}^2 \to \mathbb{R} \cup \{+\infty\}$ is defined as

$$F(t, Z, V, \alpha, \beta) := \begin{cases} H(\beta_{11}, V, \bar{\eta}^2 V) & \text{if } (\alpha, \beta) \in \Gamma(t, V), \\ +\infty & \text{otherwise,} \end{cases}$$
 (21)

where the convex set Γ is defined as

$$\Gamma(t,V) := \{(\alpha,\beta) \in \mathbb{R}^2 \times \mathbb{S}^2 \mid \alpha_1 = r(t) - q(t) - \beta_{11}/2, \ \alpha_2 = \kappa(\theta - V), \ \beta_{12} = \beta_{21} = \bar{\eta}\xi V, \ \beta_{22} = \xi^2 V \}.$$

Remark 4.4. The function H penalises deviations of the LSV model from a pure Heston model by choosing $\bar{x} = V$ (see Remark 4.1). This approach seeks to retain the attractive features of the Heston model while still matching all the market prices. We also set $s = \bar{\eta}^2 V$ to ensure that $\sigma^2 > \bar{\eta}^2 V$, hence β remains positive definite and the correlation η is in [-1,1]. The set Γ forces X_t to have dynamics of the form (17) with η defined in (20) by restricting the characteristics in Γ . In particular, it remains risk neutral.

By applying Proposition 3.5, the dual formulation of (19) with the cost function (21) is as follows:

$$\mathcal{V} = \sup_{\lambda \in \mathbb{R}^m} \sum_{i=1}^m \lambda_i c_i - \phi(0, Z_0, V_0), \tag{22}$$

where ϕ is the viscosity solution to the HJB equation

$$\partial_t \phi + \sum_{i=1}^m \lambda_i G_i \delta_{\tau_i} + \sup_{\beta_{11}} \left\{ (r - q - \frac{1}{2}\beta_{11}) \partial_Z \phi + \kappa(\theta - V) \partial_V \phi + \bar{\eta} \xi V \partial_{ZV} \phi \right.$$

$$\left. + \frac{1}{2}\beta_{11} \partial_{ZZ} \phi + \frac{1}{2} \xi^2 V \partial_{VV} \phi - H(\beta_{11}, V, \bar{\eta}^2 V) \right\} = 0,$$

$$(23)$$

with a terminal condition $\phi(T,\cdot)=0$.

Given any $\lambda \in \mathbb{R}^m$, we can calculate $\phi(0, Z_0, V_0)$ by numerically solving the HJB equation (23). The optimal λ can be found through a standard optimisation algorithm (see Section 5.1 below). The convergence of the algorithm can be improved by providing the gradient of the objective. Let $\bar{\beta}(\lambda)$ denotes the optimal β_{11} that solves the supremum in (23). In fact, solving the supremum in (23) is equivalent to solving the following equation for σ^2 :

$$(\partial_{ZZ}\phi - \partial_{Z}\phi)/2 = \partial_{\sigma^{2}}H(\sigma^{2}, V, \bar{\eta}^{2}V), \tag{24}$$

for which a closed-form solution is available. Then, denote by $\mathbb{P}(\lambda) \in \mathcal{P}^1$ a probability measure characterised by $(\alpha^{\mathbb{P}(\lambda)}, \beta^{\mathbb{P}(\lambda)})$ defined in (18) with $(\sigma_t, \eta_t) = (\sqrt{\bar{\beta}(\lambda)_t}, \bar{\eta}\sqrt{V_t/\bar{\beta}(\lambda)_t}), t \leq T$.

Lemma 4.5. Define $J(\lambda) = \sum_{i=1}^{m} \lambda_i c_i - \phi(0, Z_0, V_0)$. The gradient of $J(\lambda)$ with respect to λ_i can be formulated as:

$$\partial_{\lambda_i} J(\lambda) = c_i - \mathbb{E}^{\mathbb{P}(\lambda)} G_i(X_{\tau_i}), \quad \forall i = 1, \dots, m.$$
 (25)

In addition, $\mathbb{E}^{\mathbb{P}(\lambda)}G_i(X_{\tau_i}) = \phi'(0, Z_0, V_0)$ where ϕ' solves

$$\partial_t \phi' + (r - q - \frac{1}{2}\bar{\beta}(\lambda))\partial_Z \phi' + \kappa(\theta - V)\partial_V \phi' + \bar{\eta}\xi V \partial_{ZV} \phi' + \frac{1}{2}\bar{\beta}(\lambda)\partial_{ZZ} \phi' + \frac{1}{2}\xi^2 V \partial_{VV} \phi' = 0,$$
(26)

with the terminal condition $\phi'(\tau_i, \cdot) = G_i$.

Proof. Since λ appears in (23), $\phi(0, Z_0, V_0)$ is also a function of λ . Given λ and the associated $\bar{\beta}(\lambda)$, by differentiating (23) with respect to λ_i for any i = 1, ..., m and writing $\phi' = \partial_{\lambda_i} \phi$, we obtain the following PDE

$$\partial_t \phi' + (r - q - \frac{1}{2}\bar{\beta}(\lambda))\partial_Z \phi' + \kappa(\theta - V)\partial_V \phi' + \bar{\eta}\xi V \partial_{ZV} \phi' + \frac{1}{2}\bar{\beta}(\lambda)\partial_{ZZ} \phi' + \frac{1}{2}\xi^2 V \partial_{VV} \phi' = -G_i \delta_{\tau_i}.$$

$$(27)$$

It is worth noting that although $\bar{\beta}(\lambda)$ depends on $(\partial_{ZZ}\phi,\partial_Z\phi)$ via (24), $\bar{\beta}(\lambda)$ can be treated as independent of λ because of its optimality. With the terminal condition $\phi'(T,\cdot)=0$, (27) can be solved by the Feynman–Kac formula (see e.g., Karatzas and Shreve, 1991, Theorem 7.6). Thus,

$$\phi'(0, Z_0, V_0) = \mathbb{E}^{\mathbb{P}(\lambda)} G_i(X_{\tau_i}).$$

Moreover, solving (27) with $\phi'(T,\cdot) = 0$ is equivalent to solving (26) with $\phi'(\tau_i,\cdot) = G_i$. The proof is completed.

Remark 4.6. Note that $\mathbb{E}^{\mathbb{P}(\lambda)}G_i(X_{\tau_i})$ is the price of the *i*-th European option calculated by X_t under $\mathbb{P}(\lambda)$, which we refer to as the model price, and c_i is the market price. Instead of solving (27) once for each option, we can perform a Monte Carlo simulation to efficiently calculate the model prices for all options. However, for the sake of accuracy, we still choose to solve (27) in the numerical examples below. Moreover, as the gradient is decreasing to zero while the solution is moving towards the optimal solution, the optimisation process can be interpreted as matching the model X_t to market prices.

5 Numerical aspects

5.1 Numerical method

In this section, we present a numerical method for solving the dual formulation. Starting with an initial $\lambda = \lambda^0$ (e.g., setting it to a null vector), we solve the HJB equation (23) to calculate $\phi(0, Z_0, V_0)$ and hence calculate $J(\lambda^0)$. Then, J is maximised over $\lambda \in \mathbb{R}^m$ through an optimisation algorithm. In particular, we employed the L-BFGS algorithm (Liu and Nocedal, 1989)

and obtained good convergence. The optimisation process can be accelerated by providing the gradient $\nabla J(\lambda)$ which can be numerically computed by (25). We measure the optimality by the maximum absolute value on the gradient. In other words, by setting a threshold ϵ_1 , the algorithm terminates when the following stopping criterion is reached:

$$\|\nabla J(\lambda)\|_{\infty} < \epsilon_1.$$

For solving the HJB equation (23), we use an alternating direction implicit (ADI) method together with the central finite difference scheme. In the numerical examples below, we employ the Douglas scheme from In 't Hout and Foulon (2010). Given an λ , we solve the HJB equation backward. Consider a discretisation of the time interval $\{t_k\}$ such that $0=t_0 < t_1 < \cdots < t_{N_T} = T, N_T \in \mathbb{N}$. At each time step t_k , we approximate $\sigma_{t_k}^2$ by solving (24) with $\phi = \phi_{t_{k+1}}$ analytically. At t_k , with the approximated $\sigma_{t_k}^2$, the HJB equation (23) is solved by the ADI finite difference method. The idea of approximate ϕ_{t_k} and $\sigma_{t_k}^2$ by $\phi_{t_{k+1}}$ is similar to the numercal scheme in Ren et al. (2007). To handle the jump discontinuities caused by the presence of the Dirac delta terms, we can solve the HJB equation interval-wise in the interals seperated by the maturities, and the jump discontinuity can be incorporated into the terminal condition of the HJB equation in each interval. More precisely, if t_{k+1} is equal to the maturity of any calibrating options, we incorporate the jump discontinuity by adding $\sum_{i=1}^m \lambda_i G_i \mathbb{1}(t_{k+1} = \tau_i)$ to $\phi_{t_{k+1}}$. The numerical method is summarised in Algorithm 1.

Due to the non-linearity of the HJB equation, when the time step sizes are too large, it might not be accurate to simply approximate $\sigma_{t_k}^2$ by $\phi_{t_{k+1}}$ at t_k . Therefore, we slightly modify the algorithm by including an iterative step to improve the approximation of $\sigma_{t_k}^2$. In the literature, this iterative step is known as *policy iteration*, see e.g., Ma and Forsyth (2017). Specifically, at each time step t_k , we first approximate $\sigma_{t_k}^2$ by solving (24) with $\phi = \phi_{t_{k+1}}$. Next, we obtain ϕ_{t_k} by solving the HJB equation (23) with $\sigma_{t_k}^2$, and then approximate $\sigma_{t_k}^2$ again by solving (24) with $\phi = \phi_{t_k}$. This process is repeated until ϕ_{t_k} converges. For completeness, the modified numerical method with policy iteration is summarised in Appendix A.3.

Algorithm 1: LSV calibration

```
Data: Market prices of European option
    Result: A calibrated OT-LSV model that matches all market prices
 1 Set an initial \lambda
 2 do
         /* Solving the HJB equation */
         for k = N_T - 1, ..., 0 do
 3
             if t_{k+1} is equal to the maturity of any calibrating options. then  | \phi_{t_{k+1}} \leftarrow \phi_{t_{k+1}} + \sum_{i=1}^{m} \lambda_i G_i \mathbb{1}(t_{k+1} = \tau_i) 
 5
 6
             Approximate \sigma_{t_k}^2 by solving (24) with \phi = \phi_{t_{k+1}}
Solve the HJB equation (23) by the ADI method at t = t_k
 7
 8
         end
 9
         /* Calculating model prices and gradient */
         Solve (26) to calculate the model prices by the ADI method
10
         Calculate the gradient \nabla J(\lambda) by (25)
11
         Update \lambda by the L-BFGS algorithm
12
13 while \|\nabla J(\lambda)\|_{\infty} > \epsilon_1
```

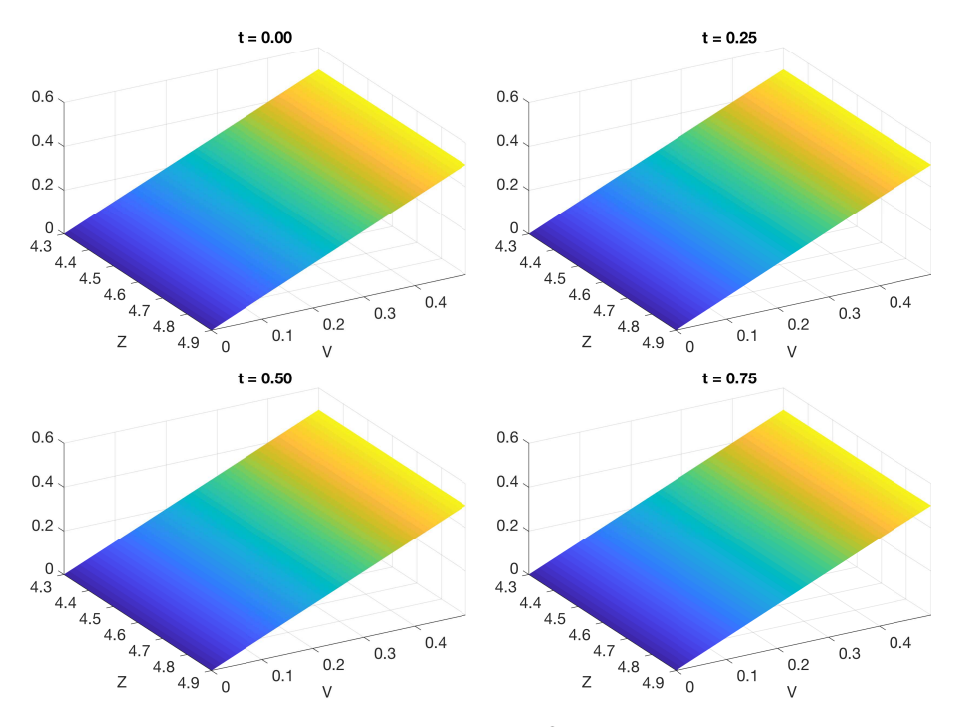


Figure 2: The volatility function $\sigma^2(t, Z, V)$ in Example 1

5.2 Numerical example: simulated data

In this section, we provide two numerical examples with simulated data to demonstrate the calibration method. In both examples, the risk-free rate is set to a constant r=0.05 and the dividend yield is set to q=0. Let $Z_0=\ln 100$ and $V_0=0.04$ for both models. We consider a uniform mesh over the computational domain $[Z_0-4\sqrt{V_0},Z_0+4\sqrt{V_0}]\times[0,0.5]$ and use 51 points for each direction. We also consider a uniform mesh over the time interval [0,1] with $N_T=100$. The LSV model is calibrated to a set of European call options generated by a Heston model with given parameters. For clarity, we will refer to the LSV model as the OT-LSV model and refer to the Heston model as the Heston generating model. The option prices are calculated at maturities in $\{0.2, 0.4, 0.6, 0.8, 1.0\}$ for strikes of all grid points in $[Z_0-1.4\sqrt{V_0}, Z_0+1.4\sqrt{V_0}]$.

5.2.1 Example 1

In the first example, we use parameters $(\kappa, \theta, \xi, \bar{\eta}) = (0.5, 0.04, 0.16, -0.4)$ for both the OT-LSV model and the Heston generating model. This example represents a trivial case, since if we use the same set of parameters for both models, the optimal solution of the dual formulation is a null vector $\lambda = \mathbf{0} \in \mathbb{R}^m$, and hence $\mathcal{V} = 0$. In this case, under the optimal measure of Problem 1, $\sigma^2(t, Z, V) = V$ and $\eta(t, Z, V) = \bar{\eta}$. Setting a threshold $\epsilon_1 = 10^{-6}$, we obtain the expected results. The plot of $\sigma^2(t, Z, V)$ is provided in Figure 2.

5.2.2 Example 2

In the second example, we give different parameters to the OT-LSV model and the Heston generating model (see Table 1). As noted in Remark 4.1, the OT-LSV model can be converted to a LV model if $\sigma^2(t, Z, V)$ is independent of V. Since it is well known that an LV model can be

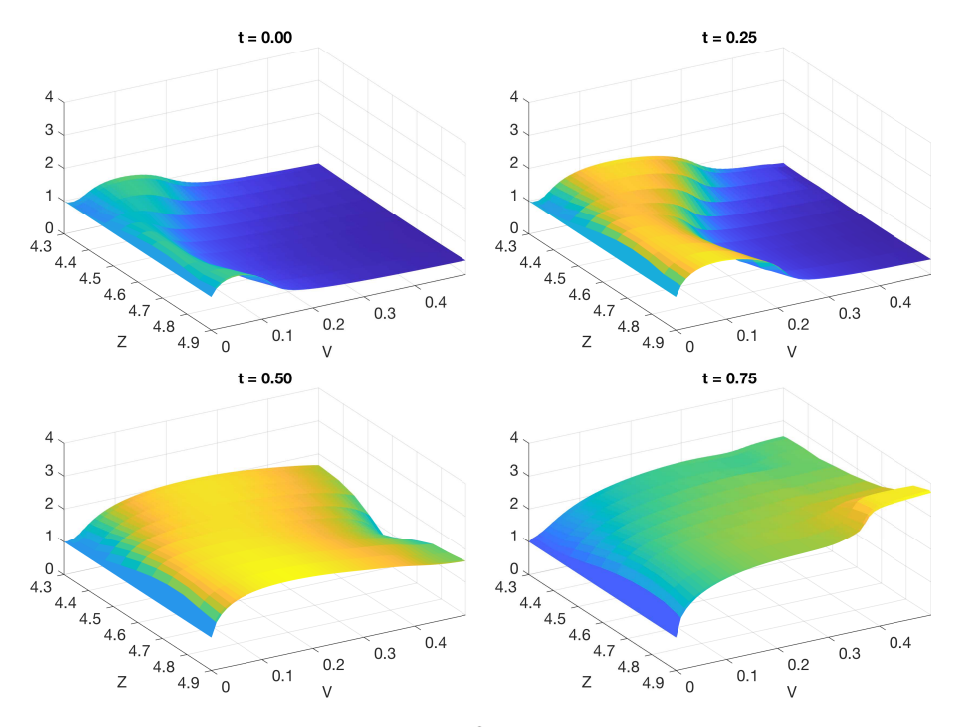


Figure 3: The function $\sigma^2(t, Z, V)/V$ in Example 2

calibrated to any arbitrage-free implied volatility surface, the calibrated OT-LSV model can exactly match all option prices generated by a Heston model. By setting the threshold $\epsilon_1=0.0005$, we obtained accurate calibration results. The calibration result for a subset of options are given in Table 2. As in the literature, the classical LSV model has $\sigma^2(t,Z,V)=L^2(t,Z)V$. Thus, we plot the function $\sigma^2(t,Z,V)/V$ in Figure 3 for comparison. The plot of the correlation function $\eta(t,Z,V)$ is also provided in Figure 4. Finally, we show the implied volatility of the Heston generated option prices and the OT-LSV generated option prices in Figure 5. We can see that the OT-LSV model is well-calibrated to the Heston generated option prices.

	κ	θ	ξ	$ar{\eta}$
Heston generating model	2.0	0.09	0.10	-0.6
OT-LSV model	0.5	0.04	0.16	-0.4

Table 1: The parameters of the Heston generating model and the OT-LSV model in Example 2

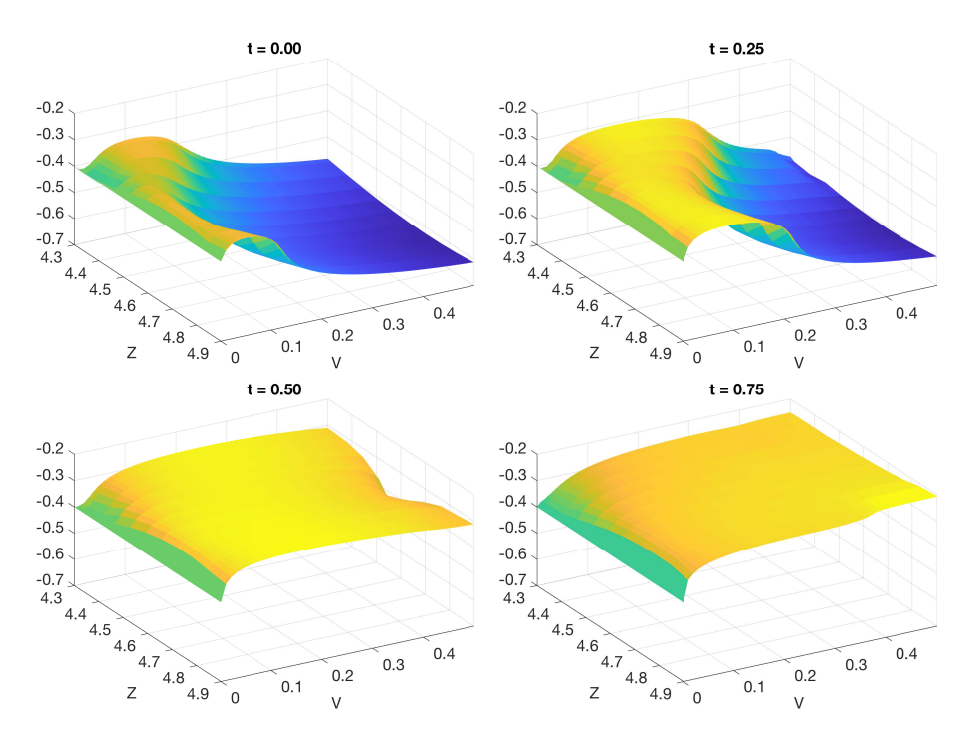


Figure 4: The correlation function $\eta(t,Z,V)$ in Example 2

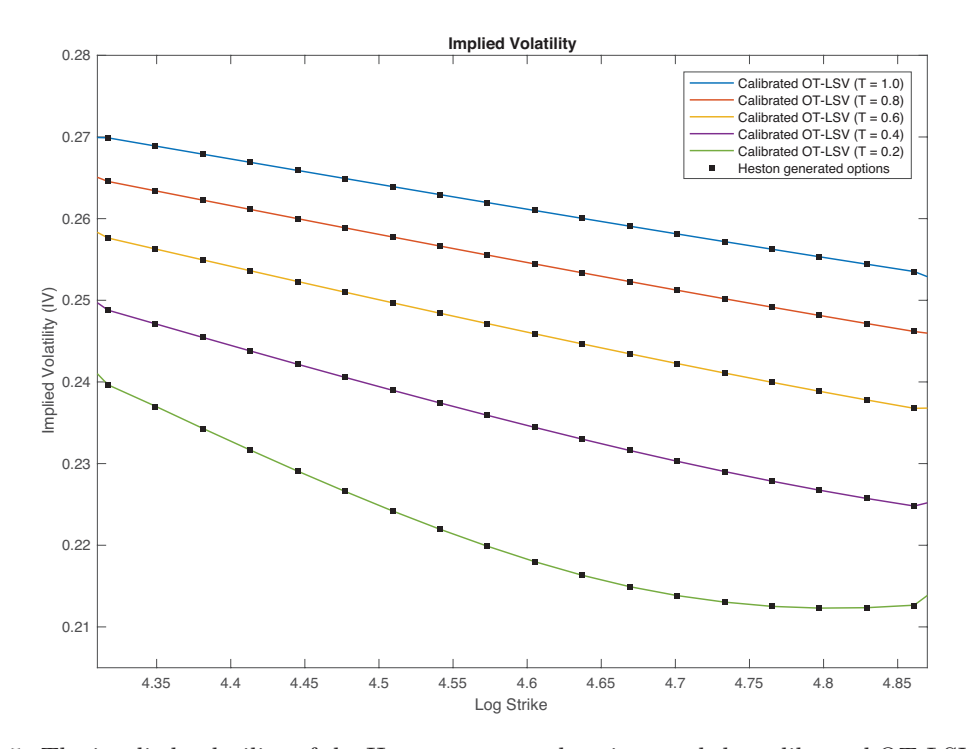


Figure 5: The implied volatility of the Heston generated options and the calibrated OT-LSV model in Example 2 $\,$

Maturity	Log-strike	Implied vol (Heston)	Implied vol (OT-LSV)	Error
	4.3492	0.2396	0.2396	5.05E-05
	4.4452	0.2291	0.2291	2.81E-06
T = 0.2	4.5732	0.2199	0.2199	4.08E-06
	4.7012	0.2138	0.2138	5.02E-06
	4.8292	0.2123	0.2124	8.48E-06
	4.3492	0.2488	0.2488	3.94E-06
	4.4452	0.2422	0.2422	1.16E-06
T = 0.4	4.5732	0.2359	0.2359	1.65E-07
	4.7012	0.2303	0.2303	9.82E-07
	4.8292	0.2257	0.2257	4.55E-06
	4.3492	0.2576	0.2576	2.84E-06
	4.4452	0.2523	0.2523	1.60E-06
T = 0.6	4.5732	0.2471	0.2471	7.56E-07
	4.7012	0.2423	0.2423	3.35E-07
	4.8292	0.2378	0.2378	3.24E-09
	4.3492	0.2646	0.2646	3.45E-06
	4.4452	0.2600	0.2600	8.69E-07
T = 0.8	4.5732	0.2555	0.2555	7.62E-07
	4.7012	0.2512	0.2512	1.42E-07
	4.8292	0.2472	0.2472	4.91E-09
	4.3492	0.2699	0.2699	8.28E-07
	4.4452	0.2659	0.2659	1.83E-06
T = 1.0	4.5732	0.2620	0.2620	1.17E-06
	4.7012	0.2581	0.2581	1.54E-06
	4.8292	0.2544	0.2544	9.24E-07

Table 2: A subset of the implied volatility of the options generated by the Heston generating model and the calibrated OT-LSV model in Example 2

5.3 Numerical example: FX market data

In this example, we calibrate the OT-LSV model to the FX options data provided in Tian et al. (2015). The options data and the domestic and foreign yields are listed in Table Appendix A.4. The parameters $(\kappa, \theta, \xi, \bar{\eta})$ are shown in Table 3, which are obtained by (roughly) calibrating a standard Heston model to the market option prices. In this case, $2\kappa\theta/\xi^2 = 0.169 \ll 1$ and the Feller condition is strongly violated.

Parameter	κ	θ	ξ	$\bar{\eta}$	Z_0	V_0
Value	0.8721	0.0276	0.5338	-0.3566	0.2287	0.012

Table 3: The parameters of the OT-LSV model in the FX market data example.

For the numerical settings, the computational domain is set on $[-0.6, 1.0] \times [0, 2]$. In order to improve the accuracy while still keeping a reasonable computation time, we employ a non-uniform mesh over the computational domain and place more points around (Z_0, V_0) (see e.g., In 't Hout and Foulon, 2010, Section 2.2.). For the time interval [0, 5], we use 30 time steps with an equal step size between any two consecutive maturities.

Setting a threshold of $\epsilon_1 = 6 \times 10^{-6}$, we obtain an exact calibration. The maximum difference between the model implied volatility and the market implied volatility is less than 1 basis point. Figure 6 shows the implied volatility of the short-maturity options (1 month and 3 months) for

the market data, the uncalibrated LSV model and the OT-calibrated LSV model. Figure 7 shows the implied volatility of the long-maturity options (2 years and 5 years).

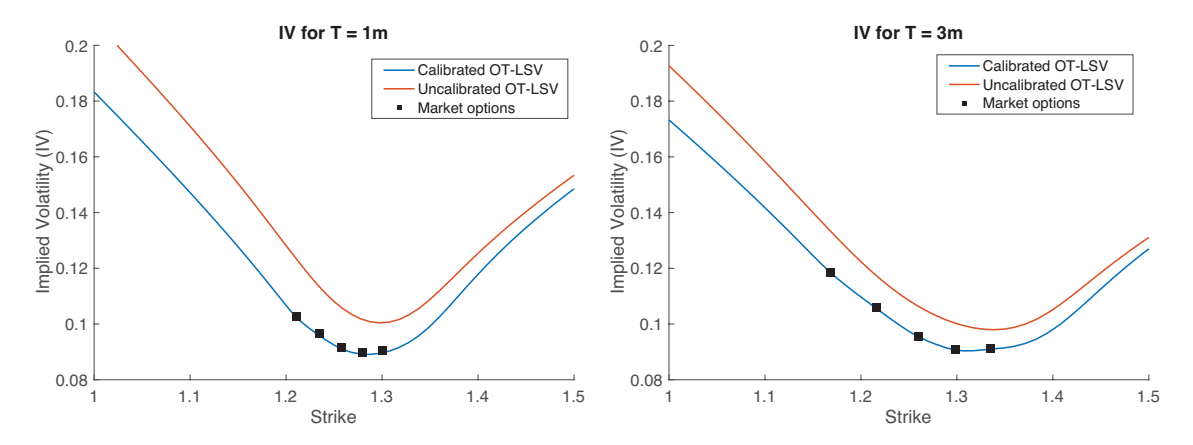


Figure 6: The implied volatility (IV) skews generated by both the uncalibrated and the calibrated OT-LSV model for 1 month and 3 months maturities in the FX market data example.

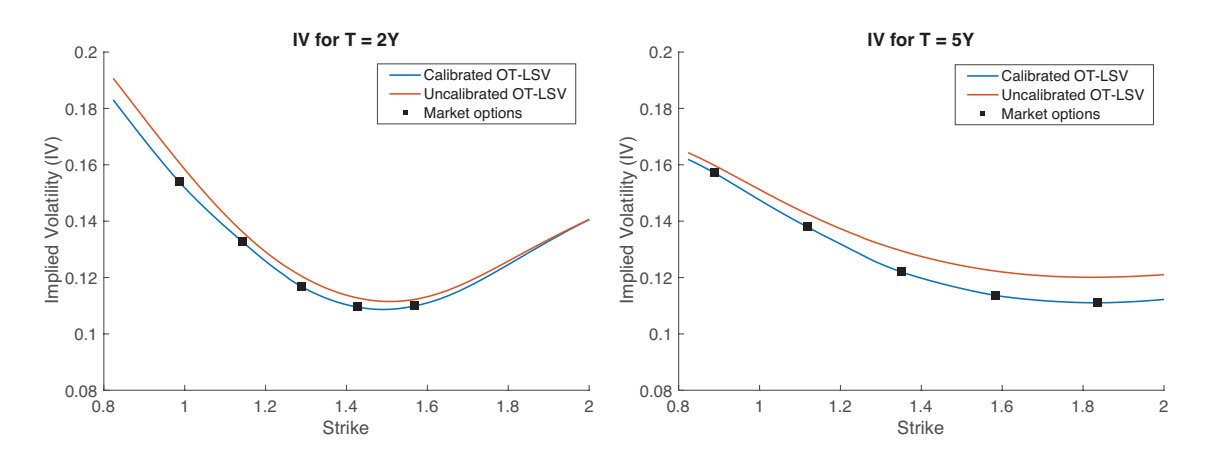


Figure 7: The implied volatility (IV) skews generated by both the uncalibrated and the calibrated OT-LSV model for 2 years and 5 years maturities in the FX market data example.

Acknowledgements

The Centre for Quantitative Finance and Investment Strategies has been supported by BNP Paribas. I. Guo has been partially supported by the Australian Research Council (Grant DP170101227). S. Wang has been supported by an Australian Government Research Training Program (RTP) Scholarship.

A Appendix

A.1 Lemma A.1

Lemma A.1. Define $\Phi: C_b(\Lambda, \mathcal{X}) \to \mathbb{R} \cup \{+\infty\}$ by

$$\Phi(r, a, b) = \begin{cases} 0 & if \ r + F^*(a, b) \le 0, \\ +\infty & otherwise. \end{cases}$$

If we restrict the domain of its convex conjugate $\Phi^*: C_b(\Lambda, \mathcal{X})^* \to \mathbb{R} \cup \{+\infty\}$ to $\mathcal{M}(\Lambda, \mathcal{X})$, then

$$\Phi^*(\rho, \mathcal{A}, \mathcal{B}) = \begin{cases} \int_{\Lambda} F\left(\frac{d\mathcal{A}}{d\rho}, \frac{d\mathcal{B}}{d\rho}\right) d\rho & \text{if } \rho \in \mathcal{M}_+(\Lambda) \text{ and } (\mathcal{A}, \mathcal{B}) \ll \rho, \\ +\infty & \text{otherwise.} \end{cases}$$

Proof. For any $(\rho, \mathcal{A}, \mathcal{B}) \in C_b(\Lambda, \mathcal{X})^*$, the convex conjugate Φ^* is given by

$$\Phi^*(\rho, \mathcal{A}, \mathcal{B}) = \sup_{(r, a, b) \in C_b(\Lambda, \mathcal{X})} \{ \langle (r, a, b), (\rho, \mathcal{A}, \mathcal{B}) \rangle \; ; \; r + F^*(a, b) \le 0 \}.$$

If we restrict the domain of Φ^* to $\mathcal{M}(\Lambda, \mathcal{X}) \subset C_b(\Lambda, \mathcal{X})^*$, then

$$\Phi^*(\rho, \mathcal{A}, \mathcal{B}) = \sup_{(r, a, b) \in C_b(\Lambda, \mathcal{X})} \left\{ \int_{\Lambda} r \, d\rho + a \cdot d\mathcal{A} + b : d\mathcal{B} \; ; \; r + F^*(a, b) \le 0 \right\}.$$

To show that ρ is a nonnegative measure, we assume that $\rho(E) < 0$ for some measurable set $E \subset \Lambda$. By the density of C_b in L^1 , there exists a sequence of functions in $C_b(\mathbb{R})$ that converges to $\mathbb{1}_E$. Let $r = -\lambda \mathbb{1}_E$ for some positive λ , $a = O^{d \times 1}$ and $b = O^{d \times d}$ where $O^{m \times n}$ denotes a null matrix of size $m \times n$. It is clear that the constraint $r + F^*(a, b) \leq 0$ is satisfied at $(-\lambda \mathbb{1}_E, O^{d \times 1}, O^{d \times d})$ as F is nonnegative. If we send λ to infinity, the function Φ^* becomes unbounded.

To show $(\mathcal{A}, \mathcal{B}) \ll \rho$, we assume that there exists a measurable set E such that $(\mathcal{A}, \mathcal{B})(E) \neq 0$ but $\rho(E) = 0$. Again, we construct a sequence of continuous functions in $C_b(\Lambda)$ converging to $\mathbb{1}_E$ in $L^1(d\rho)$. Then let $r = -F^*(a,b)$, $a = \lambda \mathbb{1}_E I^{d\times 1}$ and $b = \lambda \mathbb{1}_E I^{d\times d}$ where $I^{m\times n}$ denotes an all-ones matrix of size $m \times n$. The function Φ^* goes to infinity if we send λ to $+\infty$ or $-\infty$, depending on the sign of \mathcal{A} and \mathcal{B} on E.

Now, since the integrand is linear in (r, a, b), if Φ^* is finite, the supremum must occur at the boundary. Thus, assuming that $\rho \in \mathcal{M}_+(\Lambda, \mathcal{X})$ and $(\mathcal{A}, \mathcal{B}) \ll \rho$, we have

$$\Phi^*(\rho, \mathcal{A}, \mathcal{B}) = \sup_{r+F^*(a,b)=0} \int_{\Lambda} \left(r + a \cdot \frac{d\mathcal{A}}{d\rho} + b : \frac{d\mathcal{B}}{d\rho} \right) d\rho$$

$$= \sup_{a,b} \int_{\Lambda} \left(a \cdot \frac{d\mathcal{A}}{d\rho} + b : \frac{d\mathcal{B}}{d\rho} - F^*(a,b) \right) d\rho$$

$$= \int_{\Lambda} \sup_{a,b} \left(a \cdot \frac{d\mathcal{A}}{d\rho} + b : \frac{d\mathcal{B}}{d\rho} - F^*(a,b) \right) d\rho$$

$$= \int_{\Lambda} F\left(\frac{d\mathcal{A}}{d\rho}, \frac{d\mathcal{B}}{d\rho} \right) d\rho.$$

The interchange of the supremum and integral is made by choosing a sequence of continuous

functions $(a,b)_n$ converging to $\nabla F(\frac{dA}{d\rho}, \frac{dB}{d\rho})$, then applying the dominated convergence theorem and the fact that F^* is continuous in its effective domain. The last equality holds since the cost function F equals to its biconjugate F^{**} according to the Fenchel-Moreau theorem (see e.g., Brezis, 2011, Theorem 1.11). The proof is completed.

A.2 Lemma A.2

In this section, we prove that, the duality between spaces C_b and \mathcal{M} can be extended to the non-compact space $[0,T] \times \mathbb{R}^d$ in this particular case. A similar argument for the Kantorovich duality of the classical optimal transport was made in Villani (2003, Appendix 1.3).

Lemma A.2. Denote by K^o the set of (r, a, b) in $C_b(\Lambda, \mathcal{X})$ that can be represented by some (ϕ, λ) in $BV([0, T], C_b^2(\mathbb{R}^d)) \times \mathbb{R}^m$ (see the proof of Theorem 3.5 for the definition of 'represented'). Let $\Phi^* : C_b(\Lambda, \mathcal{X})^* \to \mathbb{R} \cup \{+\infty\}$ and $\Psi^* : C_b(\Lambda, \mathcal{X})^* \to \mathbb{R} \cup \{+\infty\}$ be defined by

$$\Phi^*(\rho, \mathcal{A}, \mathcal{B}) = \sup_{(r, a, b) \in C_b(\Lambda, \mathcal{X})} \{ \langle (r, a, b), (\rho, \mathcal{A}, \mathcal{B}) \rangle \; ; \; r + F^*(a, b) \le 0 \},$$

$$\Psi^*(\rho, \mathcal{A}, \mathcal{B}) = \sup_{(r,a,b) \in K^o} \langle (r,a,b), (\rho, \mathcal{A}, \mathcal{B}) \rangle - \int_{\mathbb{R}^d} \phi(0,x) \, d\mu_0 + \sum_{i=1}^m \lambda_i c_i.$$

Then,

$$\inf_{(\rho,\mathcal{A},\mathcal{B})\in C_b(\Lambda,\mathcal{X})^*} (\Phi^* + \Psi^*)(\rho,\mathcal{A},\mathcal{B}) = \inf_{(\rho,\mathcal{A},\mathcal{B})\in \mathcal{M}(\Lambda,\mathcal{X})} (\Phi^* + \Psi^*)(\rho,\mathcal{A},\mathcal{B}).$$
(28)

Proof. Let $C_0(\Lambda, \mathcal{X})$ be the space of continuous functions on Λ valued in \mathcal{X} that vanish at infinity. We decompose $(\rho, \mathcal{A}, \mathcal{B}) = (\tilde{\rho}, \tilde{\mathcal{A}}, \tilde{\mathcal{B}}) + (\delta \rho, \delta \mathcal{A}, \delta \mathcal{B})$ such that $(\tilde{\rho}, \tilde{\mathcal{A}}, \tilde{\mathcal{B}}) \in \mathcal{M}(\Lambda, \mathcal{X})$ and $\langle (\phi_{\rho}, \phi_{\mathcal{A}}, \phi_{\mathcal{B}}), (\delta \rho, \delta \mathcal{A}, \delta \mathcal{B}) \rangle = 0$ for any $(\phi_{\rho}, \phi_{\mathcal{A}}, \phi_{\mathcal{B}}) \in C_0(\Lambda, \mathcal{X})$ (The reader can refer to Villani (2003, Appendix 1.3) for the existence of such a decomposition.). Since, $\mathcal{M}(\Lambda, \mathcal{X})$ is a subset of $C_b(\Lambda, \mathcal{X})^*$, it follows that

$$\inf_{(\rho,\mathcal{A},\mathcal{B})\in C_b(\Lambda,\mathcal{X})^*} (\Phi^* + \Psi^*)(\rho,\mathcal{A},\mathcal{B}) \leq \inf_{(\rho,\mathcal{A},\mathcal{B})\in \mathcal{M}(\Lambda,\mathcal{X})} (\Phi^* + \Psi^*)(\rho,\mathcal{A},\mathcal{B}).$$

Next, we show that the converse of the above inequality is also valid. For Φ^* , it follows by a standard approximation argument that

$$\begin{split} \Phi^*(\rho, \mathcal{A}, \mathcal{B}) &\geq \sup_{(r, a, b) \in C_0(\Lambda, \mathcal{X})} \left\{ \langle (r, a, b), (\rho, \mathcal{A}, \mathcal{B}) \rangle \; ; \; r + F^*(a, b) \leq 0 \right\} \\ &= \sup_{(r, a, b) \in C_0(\Lambda, \mathcal{X})} \left\{ \int_{\Lambda} r \, d\tilde{\rho} + a \cdot d\tilde{\mathcal{A}} + b : d\tilde{\mathcal{B}} \; ; \; r + F^*(a, b) \leq 0 \right\} \\ &= \Phi^*(\tilde{\rho}, \tilde{\mathcal{A}}, \tilde{\mathcal{B}}). \end{split}$$

For Ψ^* , if we restrict its domain to $(\tilde{\rho}, \tilde{\mathcal{A}}, \tilde{\mathcal{B}}) \in \mathcal{M}(\Lambda, \mathcal{X})$, then $\Psi^* = -\int_{\mathbb{R}^d} \phi(0, x) d\mu_0$ if $(\tilde{\rho}, \tilde{\mathcal{A}}, \tilde{\mathcal{B}})$ satisfies the constraints (6) and (7) or $\Psi^* = +\infty$ otherwise. Whenever Ψ^* is finite,

$$\int_{\Lambda} r \, d\tilde{\rho} + a \cdot d\tilde{\mathcal{A}} + b : d\tilde{\mathcal{B}} + \sum_{i=1}^{m} \lambda_i c_i = 0 \qquad \forall (r, a, b) \in K^o.$$
 (29)

The equation (29) holds in particular for (r, a, b) in the subset $K^o \cap C_0(\Lambda, \mathcal{X})$. Thus,

$$\Psi^*(\tilde{\rho}, \tilde{\mathcal{A}}, \tilde{\mathcal{B}}) = \sup_{(r,a,b)\in K^o} \int_{\Lambda} r \, d\tilde{\rho} + a \cdot d\tilde{\mathcal{A}} + b : d\tilde{\mathcal{B}} - \int_{\mathbb{R}^d} \phi(0,x) \, d\mu_0 + \sum_{i=1}^m \lambda_i c_i$$

$$= \sup_{(r,a,b)\in K^o\cap C_0(\Lambda,\mathcal{X})} \int_{\Lambda} r \, d\tilde{\rho} + a \cdot d\tilde{\mathcal{A}} + b : d\tilde{\mathcal{B}} - \int_{\mathbb{R}^d} \phi(0,x) \, d\mu_0 + \sum_{i=1}^m \lambda_i c_i$$

$$= \sup_{(r,a,b)\in K^o\cap C_0(\Lambda,\mathcal{X})} \langle (r,a,b), (\rho,\mathcal{A},\mathcal{B}) \rangle - \int_{\mathbb{R}^d} \phi(0,x) \, d\mu_0 + \sum_{i=1}^m \lambda_i c_i$$

$$< \Psi^*(\rho,\mathcal{A},\mathcal{B})$$

where the last inequality holds since $K^o \cap C_0(\Lambda, \mathcal{X})$ is a subset of K^o . Therefore,

$$\inf_{(\rho,\mathcal{A},\mathcal{B})\in C_b(\Lambda,\mathcal{X})^*} (\Phi^* + \Psi^*)(\rho,\mathcal{A},\mathcal{B}) \geq \inf_{(\rho,\mathcal{A},\mathcal{B})\in \mathcal{M}(\Lambda,\mathcal{X})} (\Phi^* + \Psi^*)(\rho,\mathcal{A},\mathcal{B}).$$

This completes the proof.

A.3 Algorithm 2

```
Algorithm 2: LSV calibration with policy iteration
   Data: Market prices of European option
    Result: A calibrated OT-LSV model that matches all market prices
 1 Set an initial \lambda
 2 do
        for k = N_T - 1, ..., 0 do
            /* Solving the HJB equation */
            if t_{k+1} is equal to the maturity of any calibrating options then
            \phi_{t_{k+1}} \leftarrow \phi_{t_{k+1}} + \sum_{i=1}^{m} \lambda_i G_i \mathbb{1}(t_{k+1} = \tau_i)
 5
            end
            /* Policy iteration */
           Let \phi_{t_k}^{new} = \phi_{t_{k+1}}
 7
 9
               Approximate \sigma_{t_k}^2 by solving (24) with \phi = \phi_{t_k}^{old}
10
              Solve the HJB equation (23) by the ADI method at t = t_k, and set the solution
11
          to \phi_{t_k}^{new}
while \|\phi_{t_k}^{new} - \phi_{t_k}^{old}\|_2 > \epsilon_2
\phi_{t_k} \leftarrow \phi_{t_k}^{new}
12
13
14
        /* Calculating model prices and gradient */
        Solve (26) to calculate the model prices by the ADI method
15
        Calculate the gradient \nabla J(\lambda) by (25)
16
        Update \lambda by the L-BFGS algorithm
17
18 while \|\nabla J(\lambda)\|_{\infty} > \epsilon_1
```

A.4 FX options data

Maturity	Option type	Strike	Implied Vol	Maturity	Option type	Strike	Implied Vol
1m	Call	1.3006	0.0905		Call	1.4563	0.1069
	Call	1.2800	0.0898		Call	1.3627	0.1052
	Call	1.2578	0.0915	1Y	Call	1.2715	0.1118
	Put	1.2344	0.0966		Put	1.1701	0.1278
	Put	1.2110	0.1027		Put	1.0565	0.1491
	Call	1.3191	0.0897		Call	1.5691	0.1100
	Call	1.2901	0.0896		Call	1.4265	0.1096
$2\mathrm{m}$	Call	1.2588	0.0933	2Y	Call	1.2889	0.1168
	Put	1.2243	0.1014		Put	1.1421	0.1328
	Put	1.1882	0.1109		Put	0.9863	0.1540
	Call	1.3355	0.0912		Call	1.6683	0.1109
	Call	1.2987	0.0908		Call	1.4860	0.1122
$3\mathrm{m}$	Call	1.2598	0.0955	3Y	Call	1.3113	0.1200
	Put	1.2160	0.1058		Put	1.1308	0.1352
	Put	1.1684	0.1185		Put	0.9468	0.1547
	Call	1.3775	0.0960		Call	1.7507	0.1104
	Call	1.3213	0.0953		Call	1.5351	0.1127
$6\mathrm{m}$	Call	1.2633	0.1013	4Y	Call	1.3306	0.1210
	Put	1.1973	0.1145		Put	1.1226	0.1365
	Put	1.1236	0.1316		Put	0.9152	0.1554
	Call	1.4068	0.1013		Call	1.8355	0.1111
$9\mathrm{m}$	Call	1.3329	0.1005		Call	1.5835	0.1137
	Call	1.2583	0.1068	5Y	Call	1.3505	0.1220
	Put	1.1745	0.1215		Put	1.1180	0.1379
	Put	1.0805	0.1407		Put	0.8887	0.1571

Table 4: The EUR/USD option data as of 23 August 2012. The spot price $S_0=1.257$ USD per EUR. At each maturity, the options correspond to 10-delta calls, 25-delta calls, 50-delta calls, 25-delta puts and 10-delta puts

Maturity	1m	2m	$3\mathrm{m}$	6m	9m	1Y	2Y	3Y	4Y	5Y
Domestic yield	0.41	0.51	0.66	0.95	1.19	1.16	0.60	0.72	0.72	0.72
Foreign yield	0.04	0.11	0.23	0.47	1.62	0.64	0.03	0.03	0.03	0.03

Table 5: The domestic and foreign yields (in %) as of 23 August 2012.

References

- Abergel, F. and Tachet, R. (2010). A nonlinear partial integro-differential equation from mathematical finance. *Discrete Contin. Dyn. Syst.*, 27(3):907–917.
- Avellaneda, M., Friedman, C., Holmes, R., and Samperi, D. (1997). Calibrating volatility surfaces via relative-entropy minimization. *Appl. Math. Finance*, 4(1):37–64.
- Benamou, J.-D. and Brenier, Y. (2000). A computational fluid mechanics solution to the Monge–Kantorovich mass transfer problem. *Numer. Math.*, 84(3):375–393.
- Bouchard, B., Loeper, G., and Zou, Y. (2017). Hedging of covered options with linear market impact and gamma constraint. SIAM J. Control Optim., 55(5):3319–3348.
- Brenier, Y. (1999). Minimal geodesics on groups of volume-preserving maps and generalized solutions of the Euler equations. *Comm. Pure Appl. Math.*, 52(4):411–452.
- Brezis, H. (2011). Functional analysis, Sobolev spaces and partial differential equations. Universitext. Springer.
- Brunick, G. and Shreve, S. (2013). Mimicking an Itô process by a solution of a stochastic differential equation. *Ann. Appl. Probab.*, 23(4):1584–1628.
- Crandall, M. G., Ishii, H., and Lions, P.-L. (1992). User's guide to viscosity solutions of second order partial differential equations. *Bull. Amer. Math. Soc.* (N.S.), 27(1):1–67.
- Cuchiero, C., Khosrawi, W., and Teichmann, J. (2020). A generative adversarial network approach to calibration of local stochastic volatility models. arXiv preprint arXiv:2005.02505.
- Dolinsky, Y. and Soner, H. M. (2014). Martingale optimal transport and robust hedging in continuous time. *Probab. Theory Related Fields*, 160(1-2):391–427.
- Dupire, B. (1994). Pricing with a smile. Risk Magazine, pages 18–20.
- Engelmann, B., Koster, F., and Oeltz, D. (2011). Calibration of the Heston stochastic local volatility model: A finite volume scheme. https://ssrn.com/abstract=1823769.
- Figalli, A. (2008). Existence and uniqueness of martingale solutions for SDEs with rough or degenerate coefficients. *J. Funct. Anal.*, 254(1):109–153.
- Gatheral, J. (2011). The volatility surface: a practitioner's guide, volume 357. John Wiley & Sons.
- Guo, I. and Loeper, G. (2018). Path dependent optimal transport and model calibration on exotic derivatives. arXiv preprint arXiv:1812.03526.
- Guo, I., Loeper, G., Obłój, J., and Wang, S. (2020). Joint modelling and calibration of spx and vix by optimal transport. *Available at SSRN 3568998*.
- Guo, I., Loeper, G., and Wang, S. (2019). Local volatility calibration by optimal transport. 2017 MATRIX Annals, 2:51–64.
- Guyon, J. (2020). The joint s&p 500/vix smile calibration puzzle solved. Risk, April.
- Guyon, J. and Henry-Labordere, P. (2011). The smile calibration problem solved. https://ssrn.com/abstract=1885032.
- Gyöngy, I. (1986). Mimicking the one-dimensional marginal distributions of processes having an Itô differential. *Probab. Theory Relat. Fields*, 71(4):501–516.
- Han, J., Jentzen, A., et al. (2020). Algorithms for solving high dimensional pdes: From nonlinear monte carlo to machine learning. arXiv preprint arXiv:2008.13333.
- Henry-Labordere, P. (2009). Calibration of local stochastic volatility models to market smiles: A monte-carlo approach. *Risk Magazine*.
- Henry-Labordere, P. (2019). From (martingale) schrodinger bridges to a new class of stochastic

- volatility models. arXiv preprint arXiv:1904.04554.
- Henry-Labordère, P. and Touzi, N. (2016). An explicit martingale version of the one-dimensional brenier theorem. *Finance Stoch.*, 20(3):635–668.
- Heston, S. L. (1993). A closed-form solution for options with stochastic volatility with applications to bond and currency options. *Rev. Financ. Stud.*, 6(2):327–343.
- Huesmann, M. and Trevisan, D. (2019). A Benamou-Brenier formulation of martingale optimal transport. *Bernoulli*, 25(4A):2729–2757.
- In 't Hout, K. J. and Foulon, S. (2010). ADI finite difference schemes for option pricing in the Heston model with correlation. *Int. J. Numer. Anal. Model.*, 7(2):303–320.
- Jex, M., Henderson, R., and Wang, D. (1999). Pricing exotics under the smile. *Risk Magazine*, pages 72–75.
- Jourdain, B. and Zhou, A. (2020). Existence of a calibrated regime switching local volatility model. *Mathematical Finance*, 30(2):501–546.
- Kantorovich, L. V. (1948). On a problem of Monge (in Russian). Zap. Nauchn. Sem. S.-Peterburg. Otdel. Mat. Inst. Steklov. (POMI), 3:255–226.
- Karatzas, I. and Shreve, S. E. (1991). Brownian motion and stochastic calculus, volume 113 of Graduate Texts in Mathematics. Springer-Verlag, second edition.
- Krylov, N. V. (2000). On the rate of convergence of finite-difference approximations for Bellman's equations with variable coefficients. *Probab. Theory Related Fields*, 117(1):1–16.
- Lacker, D., Shkolnikov, M., and Zhang, J. (2019). Inverting the markovian projection, with an application to local stochastic volatility models. arXiv preprint arXiv:1905.06213.
- Liu, D. C. and Nocedal, J. (1989). On the limited memory BFGS method for large scale optimization. *Mathematical Programming*, 45(3, (Ser. B)):503–528.
- Loeper, G. (2006). The reconstruction problem for the Euler-Poisson system in cosmology. *Arch. Ration. Mech. Anal.*, 179(2):153–216.
- Ma, K. and Forsyth, P. A. (2017). An unconditionally monotone numerical scheme for the two-factor uncertain volatility model. *IMA Journal of Numerical Analysis*, 37(2):905–944.
- March, H. D. and Henry-Labordere, P. (2019). Building arbitrage-free implied volatility: Sinkhorn's algorithm and variants. *Available at SSRN 3326486*.
- Monge, G. (1781). Mémoire sur la théorie des déblais et des remblais. *Histoire de l'Académie Royale des Sciences de Paris*.
- Pal, S., Wong, T.-K. L., et al. (2018). Exponentially concave functions and a new information geometry. *Ann. Probab.*, 46(2):1070–1113.
- Ren, Y., Madan, D., and Qian, M. Q. (2007). Calibrating and pricing with embedded local volatility models. *Risk Magazine*, 20(9):138.
- Saporito, Y. F., Yang, X., and Zubelli, J. P. (2019). The calibration of stochastic local-volatility models: an inverse problem perspective. *Comput. Math. Appl.*, 77(12):3054–3067.
- Tan, X. and Touzi, N. (2013). Optimal transportation under controlled stochastic dynamics. *Ann. Probab.*, 41(5):3201–3240.
- Tian, Y., Zhu, Z., Lee, G., Klebaner, F., and Hamza, K. (2015). Calibrating and pricing with a stochastic-local volatility model. *Journal of Derivatives*, 22(3):21.
- Trevisan, D. (2016). Well-posedness of multidimensional diffusion processes with weakly differentiable coefficients. *Electron. J. Probab.*, 21:Paper No. 22, 41.
- Villani, C. (2003). Topics in optimal transportation, volume 58 of Graduate Studies in Mathematics. American Mathematical Society, Providence, RI.

Wyns, M. and Du Toit, J. (2017). A finite volume–alternating direction implicit approach for the calibration of stochastic local volatility models. *Int. J. Comput. Math.*, 94(11):2239–2267.